Towards coordinated regional multi-satellite InSAR volcano observations: results from the Latin America pilot project

M. E. Pritchard[1*] , J. Biggs[2], C. Wauthier[3], E. Sansosti[4], D. W. D. Arnold[2], F. Delgado[1], S. K. Ebmeier[5], S. T. Henderson[1,6], K. Stephens[3], C. Cooper[2], K. Wnuk[3], F. Amelung[7], V. Aguilar[8], P. Mothes[9], O. Macedo[8,10], L. E. Lara[11], M. P. Poland[12] and S. Zoffoli[13]

Abstract

Within Latin America, about 319 volcanoes have been active in the Holocene, but 202 of these volcanoes have no seismic, deformation or gas monitoring. Following the 2012 Santorini Report on satellite Earth Observation and Geohazards, the Committee on Earth Observation Satellites (CEOS) developed a 4-year pilot project (2013-2017) to demonstrate how satellite observations can be used to monitor large numbers of volcanoes cost-effectively, particularly in areas with scarce instrumentation and/or difficult access. The pilot aims to improve disaster risk management (DRM) by working directly with the volcano observatories that are governmentally responsible for volcano monitoring as well as with the international space agencies (ESA, CSA, ASI, DLR, JAXA, NASA, CNES). The goal is to make sure that the most useful data are collected at each volcano following the guidelines of the Santorini report that observation frequency is related to volcano activity, and to communicate the results to the local institutions in a timely fashion. Here we highlight how coordinated multi-satellite observations have been used by volcano observatories to monitor volcanoes and respond to crises. Our primary tool is measurements of ground deformation made by Interferometric Synthetic Aperture Radar (InSAR), which have been used in conjunction with other observations to determine the alert level at these volcanoes, served as an independent check on ground sensors, guided the deployment of ground instruments, and aided situational awareness. During this time period, we find 26 volcanoes deforming, including 18 of the 28 volcanoes that erupted – those eruptions without deformation were less than 2 on the VEI scale. Another 7 volcanoes were restless and the volcano observatories requested satellite observations, but no deformation was detected. We describe the lessons learned about the data products and information that are most needed by the volcano observatories in the different countries using information collected by questionnaires. We propose a practical strategy for regional to global satellite volcano monitoring for use by volcano observatories in Latin America and elsewhere to realize the vision of the Santorini report.

Keywords: Remote sensing, Latin America, InSAR

Introduction

Unlike most other types of geohazards, many volcanic eruptions are presaged by volcanic unrest lasting a few hours to years (e.g., (Passarelli and Brodsky 2012; Phillipson et al. 2013)). Unrest has been measured by satellite before several eruptions and has included

*Correspondence: pritchard@cornell.edu
[1]Department of Earth and Atmospheric Sciences, Cornell University, 112 Hollister Drive, 14850 Ithaca, NY, USA
Full list of author information is available at the end of the article

changes in surface temperature, ground deformation, and variations in the flux of gases from the volcano (e.g., (Dehn et al. 2002; Pieri and Abrams 2005; McCormick et al. 2012; Chaussard et al. 2013; Delgado et al. 2014b; Biggs et al. 2014)). It is estimated that up to 45% of the world's ~ 1400 Holocene subaerial volcanoes are unmonitored (meaning that they have no ground-based seismic, gas, or deformation monitoring: (Brown et al. 2015a,b) and space-based observations are critical for discovering and characterizing unrest at these otherwise unmonitored volcanoes. Even for those volcanoes with ground-based

Pritchard *et al. Journal of Applied Volcanology* (2018) 7:5

Page 2 of 28

instruments, satellites can provide unique complementary information. For example, during the 2010 eruption of Merapi, Indonesia, frequent satellite radar acquisitions provided critical information about the rate of dome growth, which in turn informed decisions related to evacuations that are credited with saving thousands of lives (e.g., (Pallister et al. 2013a)).

While remote sensing observations have proven their worth in volcano monitoring and are routinely being used to track activity at some volcanoes (e.g., (Tait and Ferrucci 2013)), there are still basic unanswered questions that challenge the use of satellite data for monitoring all of the world's subaerial volcanoes. For example, what remote sensing datasets are most critical for detecting changes in unrest and eruptive activity given varied styles of volcanism and diverse environmental settings? One approach would be to collect data from all relevant satellites over all of the world's volcanoes on every pass. Given limits on satellite resources and user capability, however, this is not a realistic nor an efficient strategy. To develop a pragmatic solution to the challenge, the 2012 Santorini report from the International Forum on Satellite Earth Observation (EO) and Geohazards suggested an integrated, international, global remote sensing geohazards monitoring effort for disaster risk management that would leverage the capabilities of the different satellites that can observe volcanoes (Bally 2012). The Santorini report highlighted the range of observational capabilities represented by the international satellites and brought together researchers from a range of disciplines. Specifically, the report recommended an observing strategy that would focus satellite observations at volcanoes depending on their level of activity: global background observations at all Holocene volcanoes; weekly observations at restless volcanoes and daily observations at erupting volcanoes. The Santorini report further called for 20-year sustainability and capacity-building that would increase the uptake of the satellite data by end-users who work in disaster risk reduction.

As a step towards realizing the vision of the Santorini report, the Committee on Earth Observation Satellites (CEOS), an umbrella organization of major international space agencies that is dedicated to international coordination of space-based Earth observations, initiated a series of Disaster Risk Management (DRM) pilot projects for different geohazards (volcanoes, earthquakes, floods and landslides). The goal of the pilot projects is to serve as a showcase for the international DRM community, demonstrating the importance of increased CEOS coordination, the benefits of easing data access for end users, and the potential roles of space agencies in DRM. Here, we focus on the volcano pilot, and specifically the project's work on volcanism in Latin America using satellite Synthetic Aperture Radar (SAR) data. Our aim is to illustrate the value added by SAR remote sensing data – especially in deriving insights that would not otherwise have been possible – and to define a strategy for satellite SAR observations that can be used to most efficiently and effectively track unrest and eruptions at volcanoes worldwide. We also highlight the need for strong ties between data providers, researchers, and end users to ensure that the agencies that are ultimately responsible for volcano monitoring have access to, and understanding of, those datasets that are most critical for making informed DRM decisions.

The CEOS volcano pilot project: motivation and implementation

The CEOS volcano pilot project consists of three elements: (A) a regional study of volcanic unrest and eruption in Latin America; (B) support of Geohazard Supersites and Natural Laboratories (GSNL) volcano targets; and (C) comprehensive remote sensing coverage of a significant eruptive event. Our focus in this paper is on objective A, which serves as the proof-of-concept for how an integrated, international, global remote sensing volcano monitoring effort might be implemented. We chose to focus our work on Latin America (Fig. 1), encompassing ~319 volcanoes spanning from central Mexico in the north to Chile in the south and including the Caribbean and Galápagos (e.g., (Delgado et al. 2014a; Global Volcanism Program 2017)).

Latin America was chosen as a test area because the volcanoes span a range of eruption types (notably, long-lived eruptions, discrete explosive eruptions, caldera- and dome-forming systems), ages (including 14 volcanoes which have not erupted in the Holocene, but show unrest) and environments (from desert to tropical jungles to snow-capped peaks). Previous deformation measurements in the region were representative of those recorded globally (Fig. 2), but with a larger number of detections of non-magmatic signals from regional surveys (including inter-eruptive, hydrothermal, flow deposit and fault-related signals), and some of the largest spatial footprints ever observed. Volcanic activity is abundant (there are dozens of volcanoes deforming or erupting per year) and eruptions have a strong impact on both local populations and air traffic. At the national level, there are well-established volcano observatories, but insufficient resources to effectively monitor all the volcanoes with ground-based networks, leaving an estimated 202 volcanoes unmonitored (Brown et al. 2015a). These observatories are well-placed to incorporate satellite observations into existing systems for forecasting eruptive activity and setting alert levels based on ground-based data.

To implement the Latin America Pilot Project (henceforth called LAPP), a group of satellite remote sensing
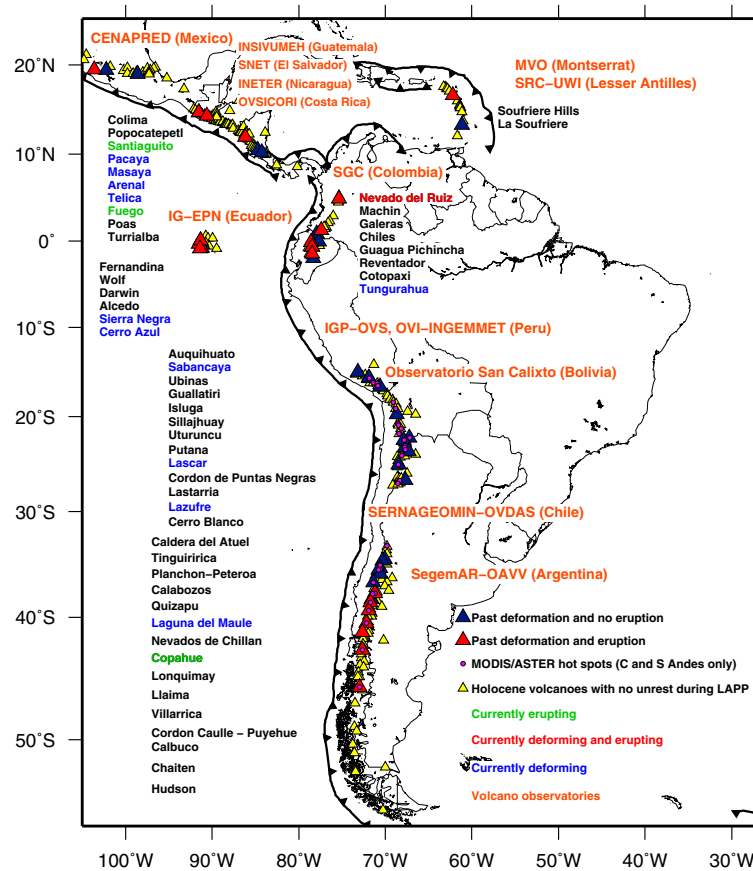
Pritchard *et al. Journal of Applied Volcanology* (2018) 7:5

Page 3 of 28

Fig. 1 Summary of ∼ 319 Latin American Holocene volcanoes from (Global Volcanism Program 2017) (yellow triangles) along with 63 volcanoes considered most active (see text) with ground deformation shown as red and blue triangles for ongoing and past deformation; ((Biggs and Pritchard 2017), and references therein), eruptions (green labels), and satellite-detected thermal anomalies as purple circles (Jay et al. 2013). Names of the volcano observatories that are responsible for monitoring the volcanoes in each country are listed in orange (acronyms are defined in Table 4)

experts was assembled. Each expert was given responsibility for a specific region, with the aim of minimizing overlap and facilitating communication with volcano observatories in each region (Fig. 1 and Additional file 1: Table S1). CEOS agencies made available hundreds of satellite images per year that would normally cost more than a million dollars (see list of satellites and space agencies in Table 1), while funding to support personnel came from a variety of sources (see Acknowledgements). To keep the size of the project manageable, the LAPP team did not include all remote sensing researchers studying volcanoes in Latin America, but team members did informally coordinate activities with non-LAPP scientists (see Acknowledgements) to extend the reach of the project and avoid duplication of effort.

The LAPP was envisioned as a 3-year project starting in late 2014 and ending in late 2017, but in this paper, we describe project work obtained using data collected

starting on 1 January 2013 (because the LAPP team used archive data) through 1 January 2017. At the initiation of the project, the following goals were established for the LAPP:

1. identification of volcanoes that are in a state of unrest in Latin America;
2. comprehensive tracking of unrest and eruptive activity using satellite data in support of hazard mitigation activities;
3. validation of Earth Observation (EO) based methodology for improved monitoring of surface deformation. Specifically, are the daily, weekly, and quarterly monitoring goals set forth by the Santorini Report sufficient to characterize volcano deformation as part of the implementation of an international, coordinated, multi-satellite volcano observing strategy? Further, what spatial resolution is needed to best monitor different types of volcanic activity;
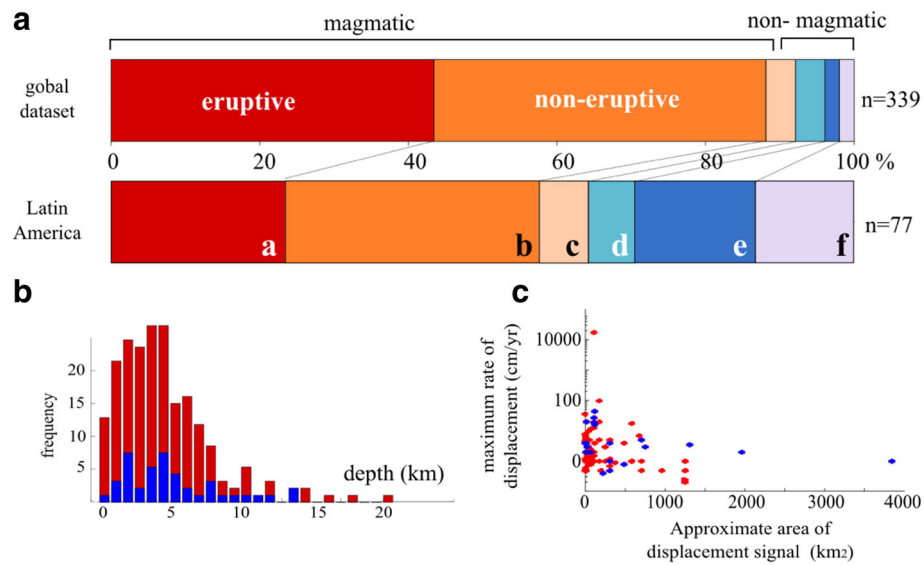
Pritchard *et al. Journal of Applied Volcanology*   (2018) 7:5

Page 4 of 28

Fig. 2 Comparison of past InSAR measurements of volcano deformation in Latin America and the rest of the world. **a**. Proportion of deformation signals attributed to co-eruptive magmatic processes (a), inter-eruptive magmatic processes (b), signals where the distinction between magmatic and hydrothermal processes is ambiguous (c), hydrothermal processes (d), flow deposit subsidence (e) and gravity-driven or faulting-related signals (f). **b**. Frequency of deformation signals according to inferred reservoir depth for Latin America (blue) and the rest of the world (red). **c**. Relationship between maximum displacement rate and approximate signal area for Latin America (blue) and the rest of the world (red)

Table 1 SAR data used in this project

Satellite(s) (Radar band)	Space agency	Quota during the LAPP	Launch date(s)	# of volcanoes
COSMO-SkyMed 1-4 (CSK) (X-band)	Agenzia Spaziale Italiana (ASI)	900	8 Jun. 2007; 9 Dec. 2007; 25 Oct. 2008; 5 Nov. 2010	16 (Santiaguito, Masaya, Turrialba, Soufriere Hills, Chiles-Cerro Negro, Wolf, Fernandina, Ubinas, Lazufre, Cerro Blanco, Laguna del Maule, Copahue, Llaima, Villarrica, Cordón Caulle, Hudson)
TerraSAR-X/TandDEM-X (TSX/TDX) (X-band)	Deutsches Zentrum für Luft- und Raumfahrt (DLR)	400	15 Jun. 2007; 21 Jun. 2010	10 (Santiaguito, Chiles-Cerro Negro, Tungurahua, Sabancaya, Ubinas, Lazufre, Laguna del Maule, Villarrica, Cordón Caulle, Hudson)
Coregistered Single look Slant range Complex (CoSSC) (X-band)	DLR	150	21 Jun. 2010	15 (Santiaguito, Pacaya, Fuego, Arenal, Nevado del Ruiz, Reventador, Ubinas, Láscar, Copahue, Llaima, Villarrica, Cordón Caulle, Chaitén, Hudson, Chaitén)
Advanced Land Observation Satellite-2 (ALOS-2) (L-band)	Japan Aerospace Exploration Agency (JAXA)	200	24 May 2014	Data available for nearly all volcanoes for the ScanSAR beam. Stripmap beam: Santiaguito, Masaya, Fernandina, Wolf, Cordón Caulle, Calbuco.
RADARSAT-2 (RSAT2) (C-band)	Canadian Space Agency/MacDonald Detwiler and Associates (CSA/MDA)	270	14 Dec. 2007	15 (Popocatepetl, Pacaya, Santiaguito, Masaya, Turrialba, Cotopaxi, Tungurahua (later became part of the supersite), Reventador, Lazufre, Laguna del Maule, Copahue, Llaima, Villarrica, Cordón Caulle, Calbuco)
Sentinel-1A/B (C-band)	European Space Agency (ESA)	No limit	3 Apr. 2014; 22 Apr. 2016	Data available for nearly all volcanoes

Pritchard *et al. Journal of Applied Volcanology*   (2018) 7:5

Page 5 of 28

4 improved EO-based monitoring of key parameters for volcanoes that are about to erupt, are erupting, or have just erupted, especially in the developing world (where in-situ resources may be scarce);

5 capacity-building in countries that do not currently have access to abundant EO data and/or the ability to process and interpret such data.

The LAPP is independent of the Group on Earth Observations (GEO) Geohazard Supersites and Natural Laboratories (GSNL) initiative (e.g., (Percivall et al. 2013); www.geo-gsnl.org), which promotes collaboration between scientists and open access to remote sensing and other data to improve understanding of volcanic and seismic hazards (e.g., (Salvi 2016)). During the course of the LAPP, an Ecaudorian volcano supersite was created covering Cotopaxi and Tungarahua volcanoes. After the Ecuadorian supersite was formed, all SAR data collected over those volcanoes became openly available to registered researchers and no longer relied on data-access through the LAPP, but the results are incorporated here for completeness.

The LAPP is also a complement to the International Charter on Space and Major Disasters which provides satellite data from multiple sensors for two weeks after selected events (www.disasterscharter.org) – for example there were five Chater activations at subaerial Latin American volcanoes during the LAPP (Copahue and Ubinas in 2013; Turrialba, Villarrica, and Calbuco in 2015). While the data are very valuable for disaster response in the short term, data are not provided in the months to years at the numerous volcanoes that exhibit unrest every year in anticipation of an event, or during crises that can last for more than two weeks.

The global satellite virtual constellation

The global satellite virtual constellation (e.g., (Wulder et al. 2015)) includes a wide range of capabilities and satellite systems. Some satellite data are routinely processed automatically in near-real time by algorithms, for example thermal detections by the Moderate Resolution Imaging Spectroradiometer (MODIS) instruments (e.g., (Wright et al. 2004)) and detections of degassing by the Ozone Monitoring Instrument (OMI) (e.g., (Krotkov et al. 2006)). Derived products are either distributed via a web-portal, or operate an alert system that sends an email to subscribed users under particular circumstances (e.g., thermal and ash detections by weather satellites, (Pavolonis et al. 2016)). Although the LAPP team made use of all available satellite resources, here we focus on SAR data, which generally lack automated processing and anomaly detection routines (but see, Hua et al. (2013); Spaans et al. (2017)).

Satellite SAR data provide two components of information about the area they image – phase and amplitude. The phase difference between two radar acquisitions separated in time and/or space is frequently used to provide information about the topography or the magnitude and spatial extent of ground deformation associated with volcanic processes and is called Interferometric Synthetic Aperture Radar (InSAR, e.g., (Bürgmann et al. 2000; Pinel et al. 2014)). In areas where the land surface changes rapidly, for example due to vegetation growth or emplacement of volcanic deposits, the phase difference observed by InSAR appears random between neighbouring pixels (incoherent), and therefore no meaningful information can be retrieved. Phase delays introduced by variation in atmospheric water vapour content can also introduce significant phase noise that can obscure or modify ground deformation signals (e.g. (Parker et al. 2015)).

In this study, SAR data were primarily used to create interferograms that record phase change related to ground deformation using the InSAR technique. In a global study using 10 years of ground-based sensors, deformation provided the longest indicators of pre-eruptive unrest (Phillipson et al. 2013); hence, InSAR is of particular interest in volcano monitoring and eruption forecasting. Increasingly, SAR data are also used to track changes in the amplitude of the radar signal to map the emplacement of volcanic deposits (e.g., (Pallister et al. 2013a; Solikhin et al. 2015; Arnold et al. 2017; Arnold et al. 2018)) and InSAR data are used to measure topographic change (e.g., (Arnold et al. (Arnold et al. 2016); Naranjo et al. (Naranjo et al. 2016); Ebmeier et al. (Ebmeier et al. 2012); Poland (Poland 2014)). We describe below how amplitude images and topographic change were used during the LAPP.

The international virtual constellation included ten SAR satellites during the lifetime of the LAPP (Table 1) with a variety of data access policies ranging from data provided at no cost to commercial missions with limited opportunities for scientific data access. While the existence of ten SAR satellites could theoretically generate significant quantities of data, only Sentinel-1a/b and Advanced Land Observation Satellite-2 (ALOS-2) collect data over all volcanoes; other satellites only collect data over a fraction of the most active or dangerous volcanoes due to trade-offs imposed by the duty cycles of the satellites (e.g., (Potin et al. 2014)). Further, imagery is not always acquired with the necessary spatial or temporal resolution to best image volcanic processes; therefore, an approach that exploits the entire international SAR virtual constellation provides the best results for detecting and characterizing volcano behaviour. For example, the spatial extent of ground deformation signals that have been detected by SAR satellites at Latin American volcanoes range from a few hundred meters (e.g., (Pavez et al. 2006; Salzer et al. 2014)) to 10 to

Pritchard *et al. Journal of Applied Volcanology*   (2018) 7:5

Page 6 of 28

100s of kilometers (e.g., (Henderson and Pritchard 2013; Feigl et al. 2013; Le Mével et al. 2015)), and so different spatial coverage and resolutions are needed to track deformation at these different extremes.

As part of the LAPP, quotas of data were allocated for SAR systems other than Sentinel-1, usually following the submission of a proposal for data access (see Acknowledgements). The quotas of data from COSMO-SkyMed (CSK), ALOS-2, and RADARSAT-2 (RSAT2) came with a data policy that did not allow for distribution of the raw data outside of the LAPP team, although derived products could be shared. A special case was data from TerraSAR-X (TSX) and TanDEM-X (TDX) satellites – data ordered by the pilot project were made openly available on the DLR supersite web portal (supersites.eoc.dlr.de), even though the volcanoes studied were not formally part of a supersite.

Topographic change associated with eruptive activity is also important for volcano monitoring (e.g., (Poland 2014; Albino et al. 2015)), so the LAPP used a second dataset of high-resolution bistatic SAR collected by the TSX and TDX satellites called Coregistered Single look Slant range Complex (CoSSC) that provides topographic information for the years 2013-2017 (Table 2). We then calculate topographic change of the CoSSCs relative to topography in February 2000 from the Shuttle Radar Topography Mission (SRTM, e.g., (Farr et al. 2007)).

Data availability and processing

We specified the observing frequency of SAR satellites needed for each of the ~ 319 Holocene-age volcanoes in Latin America motivated by the recommendations of the Santorini Report (Additional file 1: Table S1), with a few modifications. We grouped the restless and erupting categories together into a category called active (63 total in Additional file 1: Table S1) that included volcanoes with eruptions during the LAPP (28 volcanoes), seismic swarms (nine) or other satellite detected unrest (54) since 1990. While the Santorini report had the goal of daily observations for erupting volcanoes, given the constraints on data quotas and satellite capabilities, we instead aimed to have approximately weekly observations at the 63 active volcanoes. More frequent observations were obtained where feasible at the request of volcano observatories, in response to eruptions, or where short repeat intervals were needed to maintain InSAR coherence (particularly for the X-band satellites). For active volcanoes in areas with snowfall (e.g., southern Chile and Argentina), observations were only collected in the austral summer months.

In fact, only about 42 of these 63 active volcanoes were observed regularly due to limits of data availability, data quality, and data quotas, all particular to each satellite system. For the CSK constellation, we were able to request that certain volcanoes be added to the background mission, which already included 163 volcanoes globally (Sacco et al. 2015). With these additions, about 103 volcanoes in Latin America had more than 10 stripmap acquisitions, and we concentrated on 16 of these where the high spatial and temporal resolution along with favorable ground conditions (e.g., lava flows with little vegetation or lack of permanent snow cover). For TSX and TDX, about 100 volcanoes had multiple scenes acquired over them in stripmap or spotlight modes, although many fewer (about 30) had enough dates to create an InSAR time series. We used data from 10 of these volcanoes with primarily stripmap data (Table 1), while a good time series of spotlight data were collected at about seven volcanoes that were studied by others (e.g., (Salzer et al. 2014; Richter et al. 2018)). For the CoSSC data from the TSX/TDX joint mission, we concentrated on data from 15 volcanoes (Table 1) where topographic change was suspected. Following the launch of RSAT2 (Table 1), the Volcano Watch background mission included quarterly observations of 16 Decade Volcanoes (three in Latin America), increased in 2010 to the 56 volcanoes in ESA GlobVolcano Initiative (18 in Latin America), and then to 805 global volcanoes (192 in Latin America) in 2012 (Mahmood 2014). We were granted a data quota for eight of these volcanoes, including one that was covered through the Ecuadorian volcanoes GSNL project. But because several volcanoes of interest were often in the same SAR frame and a few volcanoes could be studied using data allocations from allied projects, a total of 15 volcanoes were examined with RSAT2 data (Table 1).

For the other 256 volcanoes not in the active category, background observations were collected about four times per year using the ALOS-2 satellite, which carries an L-band radar that provides better long term coherence in heavily vegetated areas and whose ScanSAR mode can acquire data over many volcanoes using relatively few scenes. Sentinel-1a/b data were used for background observations in all areas as well as to test the coherence of these data for different types of vegetation. Processing of SAR data was accomplished using a variety of methods (time series, single interferograms, and radar shadowing) and software packages (GAMMA, ROI_PAC, ISCE and GMTSAR) depending on the institution and type of data available and are described in the individual publications from the LAPP (e.g., (Muller et al. 2015; Naranjo et al. 2016; Ebmeier et al. 2016; Morales-Rivera et al. 2017; Arnold et al. 2016; Delgado et al. 2016; Henderson et al. 2017; Henderson and Pritchard 2017; Delgado et al. 2017; Wnuk and Wauthier 2017; Stephens and Wauthier 2018)). Further details are provided in the captions to the figures showing the data.

Pritchard *et al. Journal of Applied Volcanology*   (2018) 7:5

Page 7 of 28

Table 2 Selected results of InSAR analysis during the LAPP for volcanoes listed from north to south

Volcano, Country	Result from InSAR	Value of satellite data or action taken
Soufriere Hills, Montserrat	Topographic changes associated with dome growth and pyroclastic density currents (Arnold et al. 2016)	Complements ground- and aerial DEMs
Popocatepetl[a], Mexico	Deformation observed of western flank in InSAR and GPS (Solano-Rojas et al. 2017)	Continued ground monitoring
Colima, Mexico[a]	Ground deformation before Jan. 2013 explosion (Salzer et al. 2014)	Continued ground monitoring
Pacaya[ab], Guatemala	Magmatic processes, lava flow compaction and & flank motion have been detected by InSAR in 2013-1014 (Wnuk and Wauthier 2017)	Only monitoring data available beside one seismic station and sparse campaign GPS data. However, three new seismic stations were installed in 2016 and three new GPS monuments will be deployed as a result of the LAPP InSAR measurements
Santiaguito[a], Guatemala	Subsidence of deposits on the southern part of the active Caliente dome (Wauthier 2016) as previously identified by (Ebmeier et al. 2012)	Only monitoring data besides campaign tiltmeters and photogrammetry studies of the active Caliente dome (Johnson et al. 2014)
Fuego[a], Guatemala	Null results but coherence is poor even with ALOS-2 likely due to the volcano's steep slopes	Limited ground-based monitoring (only one single short-period seismometer with low signal-to-noise ratio on the eastern flank)
Masaya[ab], Nicaragua	Ground deformation due to conduit processes associated with explosive eruptions in 2012 (Stephens et al. 2017). Uplift offset from active summit during unrest in 2015-2016 (Stephens and Wauthier 2018)	Only monitoring data available, besides few seismometers and 1 GPS station in the caldera and 1 in Managua city. New GPS stations are being installed as a result of the LAPP InSAR results
Momotombo[ab], Nicaragua	Lack of pre-eruptive inflation has been confirmed by InSAR (Roman et al. 2016)	1 permanent GPS station confirms no pre-eruptive inflation (Roman et al. 2016). Those results showed there was no major shallow magma storage and thus helped INETER with hazards assessment. Additionally, following those results, new GPS instruments around the volcano are being installed
Telica[a], Nicaragua	Co-eruptive deformation in 2015 confirmed by InSAR (Diana Roman, personal communication, 2017)	1 GPS station is consistent with motion observed with InSAR data
Arenal, Costa Rica	Loading and landsliding associated with recently erupted products (Muller et al. 2015)	InSAR data provided spatial covereage needed to identify process responsible for deformation, and to detect landslides on upper slopes.
Turrialba[b], Costa Rica	GPS measured deformation associated with eruptions and long-term background uplift. No major deformation in C-band and L-band interferograms. X-band data incoherent so localised deformation around vent would be undetected.	Continued ground monitoring
Poas[b], Costa Rica	GPS measured deformation associated with phreatic eruption in 2017. No background X-band acquisitions available to provide confirmation.	Continued ground monitoring
Nevado del Ruiz, Colombia[a]	Broad uplift discovered centered 10 km SW of volcano (Lundgren et al. 2015)	Provided synoptic context to understand GPS data that only captured fraction of deformation

Pritchard *et al. Journal of Applied Volcanology* (2018) 7:5

Page 8 of 28

Table 2 Selected results of InSAR analysis during the LAPP for volcanoes listed from north to south (*Continued*)

Volcano, Country	Result from InSAR	Value of satellite data or action taken
Chiles-Cerro Negro, Colombia-Ecuador	Ground deformation during seismic crisis at unmonitored volcano (Ebmeier et al. 2016)	InSAR data added to evidence from the ground observations to assess hazard
Reventador[ab], Ecuador	Topographic change associated with ongoing eruption. TanDEM-X and RSAT2 used to map 43 independent lava flows in 2012-2016 (Naranjo et al. 2016; Arnold et al. 2017)	InSAR data critical to measuring flow thickness and hence effusion rates
Tungurahua[ab], Ecuador	Also covered by GSNL. Frequent deformation on western flank detected with multiple satellites	Dense ground-based network, but deformation located between sensors (Muller 2016).
Cotopaxi[ab], Ecuador	Also covered by GSNL. Pre-eruptive deformation (Morales-Rivera et al. 2017); co-eruptive amplitude changes (Arnold et al. 2018).	Amplitude images confirmed changes in ice-cap detected by overflights. Pre-eruptive deformation detected retrospectively.
Fernandina, Ecuador	InSAR time series shows continuous uplift over the 2012-2013 period only shortly interrupted for a couple of months at the end of 2012 (Pepe et al. 2017).	Continued limited ground monitoring (1 working seismometer)
Wolf[a], Ecuador	InSAR time series shows large co-eruptive ground deformation and confirms results based on single interferograms, as in (Xu et al. 2016). No clear evidence of pre-eruptive deformation signals.	No ground monitoring, but for some seismometers on nearby islands (Bernard et al. 2015)
Auquihuato, Perú	Earthquake deformation at unmonitored volcano (Morales-Rivera et al. 2016) although no deformation observed 4/14-7/16	Ground observations planned for future
El Misti, Perú	No deformation associated with media reports of increased activity	Continued ground monitoring
Ticsani, Perú	No deformation during earthquake swarms (June-Sept. 2015)	Continued ground monitoring
Sabancaya[ab], Perú	Earthquake deformation, but no large magmatic signal (Jay et al. 2015) until potential signal in 2015-2016 (Additional file 2: Figure S2)	Combined with ground measurements during ongoing crisis
Ubinas[ab], Perú	No ground deformation measured spanning several eruptions (Additional file 2: Figure S3)	Lack of deformation is not understood
Guallatiri[b], Chile	Ground sensor detected motion but InSAR didn't (Additional file 2: Figure S4)	Ground sensor determined to be malfunctioning
Uturuncu, Bolivia	Continued deformation detected by ground sensors but not sufficient InSAR between 2010-2014 (Henderson and Pritchard 2017)	No action
Láscar[a], Chile	Crater subsidence unaffected by VEI 1-2 eruptions (Richter et al. 2018)	Continued ground monitoring
Lazufre, Chile-Argentina	Deformation rate slowed down (Henderson et al. 2017)	Continued ground monitoring
Cerro Blanco, Argentina	Continued subsidence (López et al. 2016)	No action
Planchón-Peteroa[b], Chile	No deformation during earthquake swarm (Additional file 2: Figure S5)	Continued ground monitoring
Laguna del Maule, Chile	Uplift confirmed by ground observations (Le Mével et al. 2015; Grainger 2017)	Continued ground monitoring
Nevados de Chillán[ab], Chile	No deformation during earthquakes or explosions	Continued ground monitoring

Pritchard *et al. Journal of Applied Volcanology* (2018) 7:5

Page 9 of 28

Table 2 Selected results of InSAR analysis during the LAPP for volcanoes listed from north to south (*Continued*)

Volcano, Country	Result from InSAR	Value of satellite data or action taken
Copahue[a], Argentina-Chile	InSAR time series show 2011-2016 inflation before summit activity (Velez et al. 2016) unaffected by several VEI 1-2 eruptions (Lundgren et al. 2017)	Continued ground monitoring
Llaima, Chile	Background observations show no deformation (Delgado et al. 2017)	Continued ground monitoring
Villarrica[ab], Chile	Deformation detected after 2015 eruption (Delgado et al. 2017)	Combined with GPS data, alert level of volcano raised
Cordón Caulle, Chile	Discovered fast uplift following eruption not detected by seismic network (Delgado et al. 2016; Euillades et al. 2017)	Deployed additional GPS receivers
Calbuco[ab], Chile	Co-eruptive but not pre-eruptive deformation (Delgado et al. 2017; Nikkhoo et al. 2017), post eruptive deformation suggested by ground sensor but not confirmed by InSAR (Additional file 2: Figure S1)	Confirmed single ground sensor had co-eruptive deformation and showed post-eruptive sensor unreliable
Chaitén, Chile	Background observations show no subsurface deformation, but topographic change at lava dome (Fig. 9e)	Continued ground monitoring
Hudson[b], Chile	Background observations show no deformation during earthquake swarm, but new CoSSC data reveal significant topographic change before 2012 (Fig. 9C)	Continued ground monitoring

[a]Volcanoes that erupted during the LAPP. [b]Volcanoes where specific observations were requested by the volcano observatory (17)

Results
Utility of satellite observations to volcano observatories during the LAPP
Table 2 summarizes the results of InSAR data analysis from 36 volcanoes from the LAPP and allied projects. These observations include the outcome of processing requests from the volcano observatories (including null results – 14 different volcanic episodes) as well as background monitoring. During the 4-year time period of the pilot discussed here, 28 different subaerial volcanoes had 43 eruptions (VEI 0-4) in Latin America that were recorded by Global Volcanism Program (2017). Not all of these eruptions were studied by the LAPP because the volcano observatories did not request satellite data, the eruptions were small, the volcanoes were already well monitored, or for another reason.

Using the information in Table 2, we summarize below the different ways the results have been used by the volcano observatories to complement the mostly ground-based monitoring already being done:

Responding to seismic crises
The LAPP frequently responded to requests from volcano observatories to provide satellite data to complement ground-based measurements of unrest. In particular, InSAR observations were often requested to assess whether there was evidence of large magma accumulation during a seismic crisis, or to confirm observations of

deformation from a single sensor. Observations from the LAPP have shown a lack of magma-driven deformation during crises at Chiles and Cerro Negro de Mayasquer (hereaftercalled Chiles-Cerro Negro), Momotombo, Sabancaya and Nevados de Chillán (Jay et al. 2015; Ebmeier et al. 2016; Roman et al. 2016), and have consequently been instrumental in the decision not to raise the alert level. In contrast, at Villarrica and Calbuco, satellite observations spanning the eruption confirmed ground results showing uplift or subsidence, which gave confidence to the decision to keep the alert level high (Delgado et al. 2017). At Guallatiri and Calbuco post-eruptive satellite observations showed that ground sensors were faulty.

The period of unrest at Chiles-Cerro Negro, which lies on the border between Ecuador and Colombia, provides an excellent example of the contribution of the LAPP during a seismic crisis. The regional seismic network first detected seismicity in October 2013, at which time the volcano had no dedicated ground-based monitoring. With a second swarm in February-May 2014, the local observatories – Instituto Geofisico-Escuela Politecnica Nacional (IG-EPN) in Ecuador, Servicio Geologico in Colombia (SGC) and Observatorio Vulcanologico y Sismologico de Pasto (OVSP) gradually installed ground-based monitoring, but also requested satellite data from the LAPP. At this time, SAR interferograms revealed negligible surface deformation (Ebmeier et al. 2016). In October 2014, a third, more intense swarm occurred, with some of the

Pritchard *et al. Journal of Applied Volcanology* (2018) 7:5

Page 10 of 28

larger earthquakes being felt in local towns. This swarm peaked on 20 October with a Mw 5.6 earthquake which caused significant damage to buildings (e.g., (Ebmeier et al. 2016)). Such large earthquakes are often considered to be a sign of impending eruption, but the event was only recorded by two GPS receivers at distances of 2 km and 15 km from the edifice, and gave limited information about the source. However, interferograms generated from TSX and CSK data as part of the LAPP showed uplift ∼5 km south of the volcano. Source modelling showed that this was consistent with an oblique thrust earthquake occurring on the El Angel fault system rather than magma accumulation, and was thus not indicative of an impending eruption. These observations played a key role in the decision to reduce rather than elevate the alert level for the volcano.

Complementing limited ground-based networks during eruptions

At Pacaya, the InSAR observations are effectively the only systematic deformation monitoring data available to complement a single seismometer. Besides the previously identified flank motion in 2010 and lava flow subsidence using ALOS-1 and UAVSAR (Schaefer et al. 2016), new RSAT2 data processed in this project provided evidence for deformation induced by magmatic processes, as well as a new episode of flank motion associated with eruptions in early 2014 (Wnuk and Wauthier 2017). Following those new InSAR results from the LAPP, the deployment of three new GPS receivers colocated with seismic stations are planned by INETER in collaboration with external partners from Michigan Tech, to complement sparse and discontinuous campaign GPS observations.

Telica in Nicaragua is classified as a persistently restless volcano. Ebmeier et al. (2013b) found no evidence for deformation using ALOS-1 InSAR data spanning 2007-2010. In 2015-2016, Telica experienced a particularly energetic eruptive episode including numerous explosions, primarily during May, September, and November 2015. Large volcanic bombs reached areas up to one kilometer away from the vent, putting local residents in danger, as well as damaging property and livestock. Unusual changes in the volcano seismicity and inner crater morphology were documented leading up to the eruption (Diana Roman, personal communication, 2017). One GPS station on the volcano showed evidence for small precursory and syn-eruptive deformation of the edifice (a few centimeters in North-South and East-West components (Pete LaFemina, personal communication, April 2017), which was not observed at Telica before. New Sentinel-1 InSAR results from the LAPP confirm the motion observed in the GPS data (Diana Roman, personal communication, 2017).
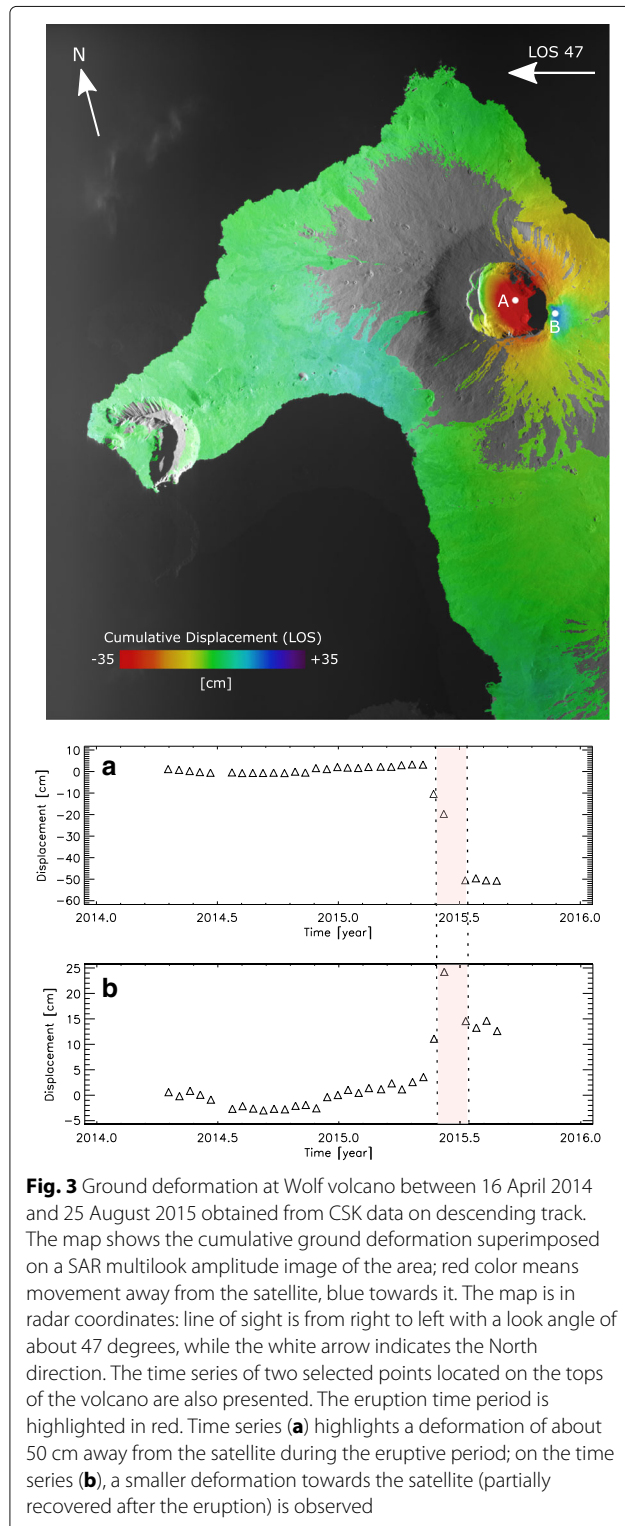
No ground-based monitoring

During the LAPP, we were able to monitor volcanoes with no ground-based networks closer than 10 km and discovered activity previously undetected. Specifically, the LAPP discovered inflation at Cordón Caulle, Chile after the end of the 2011-2012 eruption that was not associated with any change detected by the regional seismic networks (Delgado et al. 2016; Euillades et al. 2017). The Chilean volcano observatory installed three new campaign GPS stations during February-April 2016 at Cordón Caulle as a result of the LAPP. Ground deformation was also discovered at the Holocene Cerro Auquihuato volcano in Perú during 2007-2011 (Morales-Rivera et al. 2016), and the discovery was communicated to the Peruvian volcano observatory during the LAPP. Cerro Auquihuato has no historic eruptions and is not monitored on the ground, but future ground measurements are planned by the Peruvian volcano observatory.

Wolf volcano, in the Galápagos Islands, is also poorly monitored; the first information on the 2015 eruption relied on a few seismic stations (one located on the Fernandina Island, 35 km to the SSW of the volcano) and on pictures taken by the crew of a cruise ship sailing the area. Only when the ash plume was formed and reached more than 10 km in altitude, was it detected by the Washington Volcanic Ash Advisory Center (Bernard et al. 2015). Sentinel-1 and CSK were acquiring data regularly at the eruption time, with a repeat time of 12 and 16 days, respectively. A few ALOS-2 acquisitions were also available. In particular, three Sentinel-1 and one ALOS-2 interferograms spanning the eruption have been used to model the active magmatic sources (Xu et al. 2016). CSK provided the best time series of ground deformation spanning the eruption (Fig. 3); in this case 30 images acquired between 16 April 2014 and 25 August 2015 on a descending track were combined through the Small BAseline Subset (SBAS) approach to compute the cumulative ground deformation map and deformation time series for each coherent pixel of the area. The map clearly shows that the largest deformation occurred on the top of the volcano. The time series of points A and B in the map also show that, in time, the deformation occurred mostly across the eruption, with only a small signal before its start that may be an atmospheric artifact.

Spatial gaps in ground-based networks

Many active volcanoes in Latin America have well-developed ground-based monitoring systems, but these are often of limited spatial extent, and are difficult to maintain during eruptions or at high elevations near summits. Satellite imagery is therefore vital to fill in spatial gaps and provide a critical synoptic perspective. The spatial coverage of InSAR data is particularly important in constraining models of the deformation source,

Pritchard *et al. Journal of Applied Volcanology* (2018) 7:5

Page 11 of 28

Fig. 3 Ground deformation at Wolf volcano between 16 April 2014 and 25 August 2015 obtained from CSK data on descending track. The map shows the cumulative ground deformation superimposed on a SAR multilook amplitude image of the area; red color means movement away from the satellite, blue towards it. The map is in radar coordinates: line of sight is from right to left with a look angle of about 47 degrees, while the white arrow indicates the North direction. The time series of two selected points located on the tops of the volcano are also presented. The eruption time period is highlighted in red. Time series (**a**) highlights a deformation of about 50 cm away from the satellite during the eruptive period; on the time series (**b**), a smaller deformation towards the satellite (partially recovered after the eruption) is observed

section (Ebmeier et al. 2016). Other examples during the LAPP include Calbuco (Delgado et al. 2017), Tungurahua and Nevado del Ruiz. The deformation at Tungurahua is localized on the western flank and lies between the GPS sites that make up the monitoring network – it was first detected in 2008 by InSAR (Fournier et al. 2010; Biggs et al. 2010), but was detected repeatedly during the LAPP (Muller 2016; Hickey et al. 2017). At Nevado de Ruiz, the GPS network detected uplift and northward motion at all sites, an observation that is difficult to interpret in terms of the magmatic plumbing system located vertically beneath the summit. InSAR observations demonstrated that there was a large, deep zone of magma accumulation located to the south of the volcano, demonstrating the importance of synoptic satellite observations in understanding the extent of deformation patterns, particularly when they are offset from the surface edifice (e.g., (Lundgren et al. 2015; Londono 2016)).

Null results and eruptions without measured deformation

For volcanoes that apparently erupt without deformation, a key question is whether the deformation is being missed because the temporal and spatial resolution of the sensors cannot capture the temporal and spatial characteristics of deformation (e.g., (Biggs and Pritchard 2017)). Tilt meters located close to volcanic vents record deformation over timescales of minutes to hours, which may occur cyclically (e.g., (Voight et al. 1999; Johnson et al. 2014; Anderson et al. 2015)) or prior to Vulcanian eruptions (Iguchi et al. 2008; Gottsman et al. 2011) install and maintain. Although these timescales remain much shorter than satellite repeat times, high spatial and temporal resolution data from X-band satellites can identify shallow conduit processes on timescales and lengthscales much shorter than earlier C-band and L-band satellites (Salzer et al. 2014; Ebmeier et al. 2014; Stephens et al. 2017). Because the LAPP uses satellite observations from a range of different platforms with different spatial and temporal resolutions, it provides a particularly good opportunity to investigate such systems.

Of the 28 subaerial eruptions that occurred during the LAPP, deformation at 18 of these was detected before, during, and/or after the eruptions (Table 2). At the other 10 volcanoes (Table 3), no deformation was observed before, during, or after the eruptions, but the eruptions were relatively small (VEI 2 or less). The volcanoes with VEI 3 (Tungurahua) and 4 (Calbuco, Wolf) eruptions during the LAPP all had detected deformation. Further, several of these volcanoes (e.g., Santiaguito, Fuego, Ubinas, Villarrica) are open systems and so the eruptions may have only a small cyclical deformation signal lasting a few minutes close to the vent that is hard to detect with InSAR observations separated by several days (e.g., (Johnson et al. 2014)).

something that is not possible to do accurately based on data from just one or two ground sensors.

The use of InSAR data in this way at Chiles-Cerro Negro was described in "Responding to seismic crises"

Pritchard *et al. Journal of Applied Volcanology* (2018) 7:5

Page 12 of 28

Table 3 Volcanoes that erupted during the LAPP but did not have clear observed InSAR deformation

Volcano	Eruption duration (max VEI)
San Miguel, El Salvador	2013-2014 (VEI 2); 2015 (VEI 1); Jan and June 2016 (VEI 1)
San Cristobal, Nicaragua	2013 (VEI 1) 2014 (VEI 1); 2015 (VEI 2); 2016 (VEI 2)
Santiaguito, Guatemala	1922-ongoing (VEI ?)
Fuego, Guatemala	2002-ongoing (VEI 2)
Rincon de la Vieja, Costa Rica	2012 (VEI 1); 2014 (VEI 1); 2015-2016 (VEI 1)
Poas, Costa Rica	2009-2014 (VEI 1); 2016 (no VEI)
Turrialba, Costa Rica	2013 (VEI 2); 2014 (VEI 2); March-May and Oct. 2015 (VEI 2) 2016-ongoing (VEI 2)
Galeras, Colombia	2012-2014 (VEI 2)
Sangay, Ecuador	1934-ongoing (VEI ?)
Nevados de Chillán, Chile	2015-2017 (VEI 2)

InSAR data quality for different satellites in different areas

Utility of Sentinel-1 C-band data for background observations

The Sentinel-1 mission represents a major step forward in terms of volcano observation, and is yielding new results thanks to its frequent repeat and global acquisition strategy. We describe areas where Sentinel-1 observations are proving useful, even in challenging environments (e.g., 12 day pairs at the higher elevation tropical volcanoes of Colombia, Fig. 4). In many cases, the rocky volcanic edifices themselves are coherent, but the densely vegetated regions surrounding them are not (e.g., San Miguel in El Salvador in and Telica, Cerro Negro and San Cristobal in Nicaragua). Multilooking and filtering data can improve coherence, however, this reduces the spatial resolution, and limits the ability to measure localized deformation signals.

However, in other areas, a different observing strategy than that currently used by Sentinel-1 might be needed to produce coherent measurements. For example, VV polarization data acquired every 12-24 days (or 35 days for ENVISAT) is often incoherent in vegetated areas (Figs. 5, 6, and Additional file 2: Figure S6) at the most dangerous volcanoes in southern Chile (including Nevados de Chillán, Villarrica, Calbuco, Cordón Caulle, Copahue) and Central America (including Fuego and Santiaguito, Guatemala as well other areas shown by Funning and Garcia (2017)). In some cases, better data quality can be obtained with shorter time period observations or using HH polarization with higher bandwidth, which provides higher spatial resolution (e.g., RSAT2 or ENVISAT extended mission, Fig. 7). An example of the superior data quality for different satellites with different
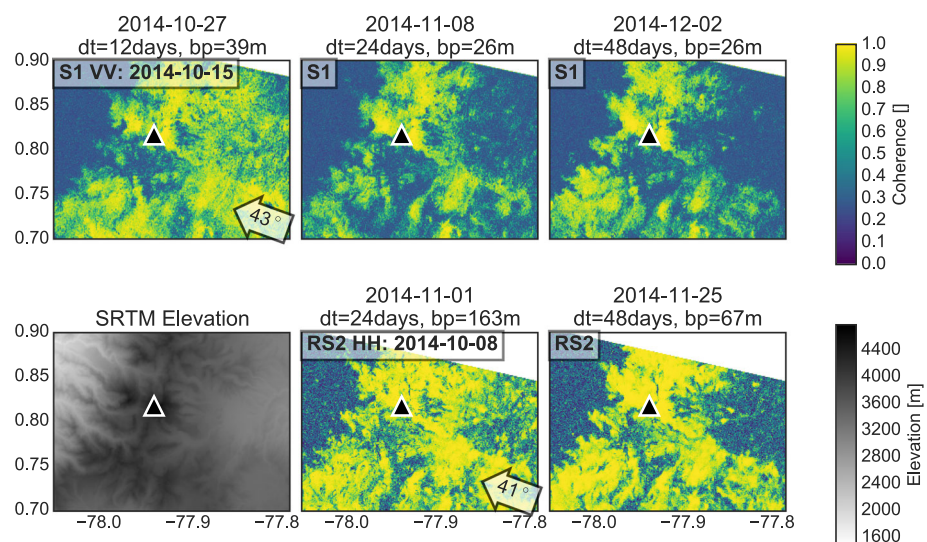
Fig. 4 Coherence (unitless) of different interferograms over Chiles-Cerro Negro on the Colombia-Ecuador border. Top row: From Sentinel-1, VV-polarized interferograms spanning 12 to 48 days, with the time span and perpendicular baseline listed. Bottom row: Topographic relief from SRTM as well as two HH=polarized RSAT2 interferograms
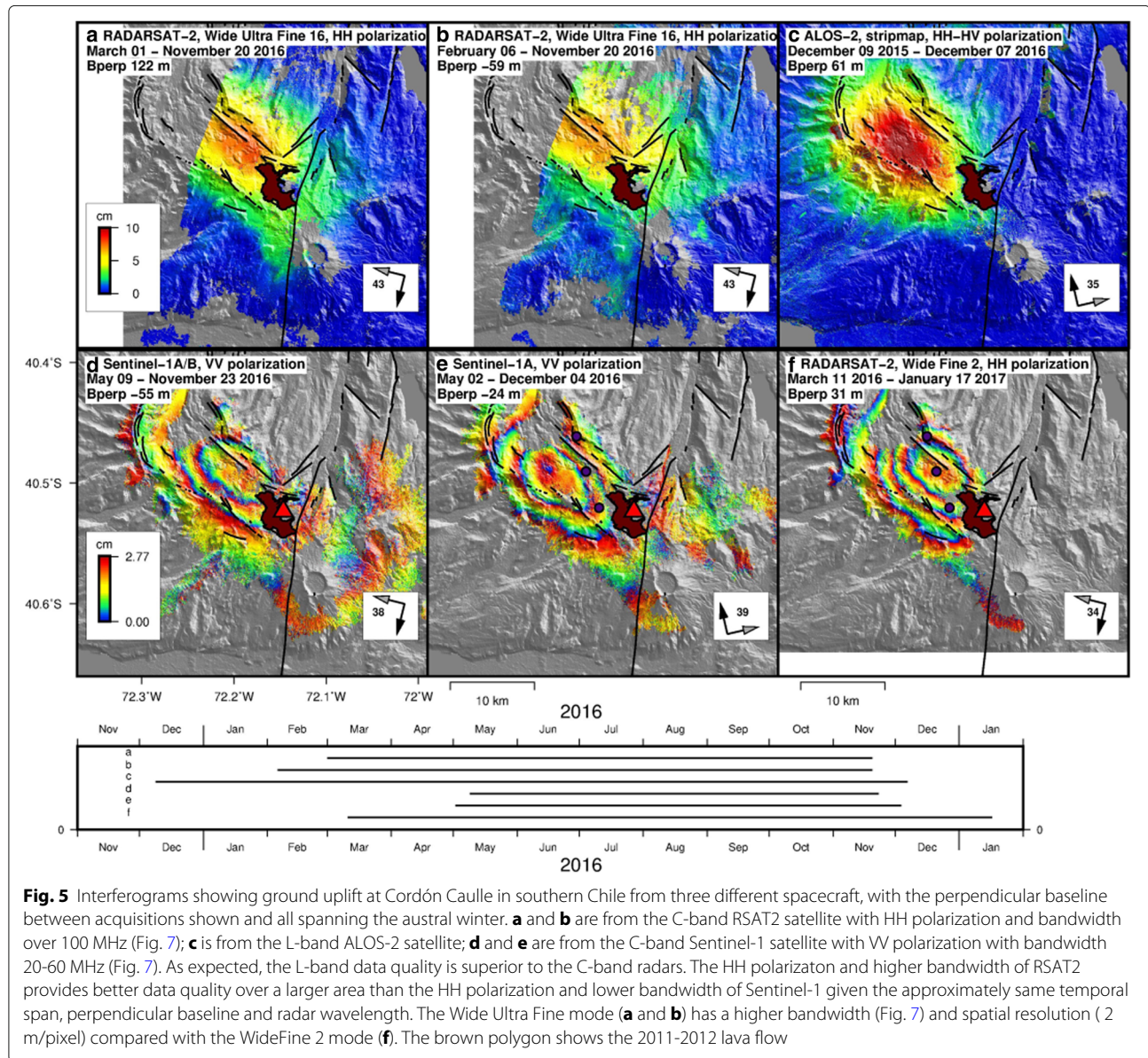
Pritchard *et al. Journal of Applied Volcanology* (2018) 7:5

Page 13 of 28

Fig. 5 Interferograms showing ground uplift at Cordón Caulle in southern Chile from three different spacecraft, with the perpendicular baseline between acquisitions shown and all spanning the austral winter. **a** and **b** are from the C-band RSAT2 satellite with HH polarization and bandwidth over 100 MHz (Fig. 7); **c** is from the L-band ALOS-2 satellite; **d** and **e** are from the C-band Sentinel-1 satellite with VV polarization with bandwidth 20-60 MHz (Fig. 7). As expected, the L-band data quality is superior to the C-band radars. The HH polarizaton and higher bandwidth of RSAT2 provides better data quality over a larger area than the HH polarization and lower bandwidth of Sentinel-1 given the approximately same temporal span, perpendicular baseline and radar wavelength. The Wide Ultra Fine mode (**a** and **b**) has a higher bandwidth (Fig. 7) and spatial resolution (2 m/pixel) compared with the WideFine 2 mode (**f**). The brown polygon shows the 2011-2012 lava flow

bandwidths and polarizations spanning the austral winter at Cordón Caulle, Chile is shown in Fig. 5. The VV polarization from Sentinel-1 is able to capture some of the ground deformation pattern, but because it is incoherent in the vegetated areas around the volcano, there is a greater ambiguity as to the cause, spatial wavelength, and amplitude of the deformation signal than from the HH C-band and L-band observations. In an effort to compare the effects of polarization and radar bandwidth on coherence at Cordón Caulle, we compared several different observation modes from different C-band radar satellites (Fig. 7). The figure shows that data from high resolution and HH polarization C-band platforms have the highest coherence at Cordón Caulle, although the exact reasons are currently under investigation. Delgado et al. (2017) reached

the same conclusion of the higher coherence of the HH ENVISAT IM6 beam compared with VV ENVISAT IM2 for nearby Llaima, Villarrica and Calbuco volcanoes.

Another example where the coherence of a HH polarized 24-day RSAT2 interferogram is superior to a 24-day VV-polarized Sentinel-1 interferogram is shown in Fig. 4 at Chiles-Cerro Negro, on the Colombia-Ecuador border. The 24 day RSAT2 interferogram is also more coherent than a 12-day Sentinel-1 VV polarized interferogram. In summary, in areas with heavy vegetation like Central America and southern Chile in Latin America as well as the Western Rift of Africa and Papua New Guinea (e.g. (Nobile et al. 2017; Garthwaite et al. 2017)), Sentinel-1 observations need to be taken every 6 days to maintain coherence. Where this is not possible, RSAT2 and L-band
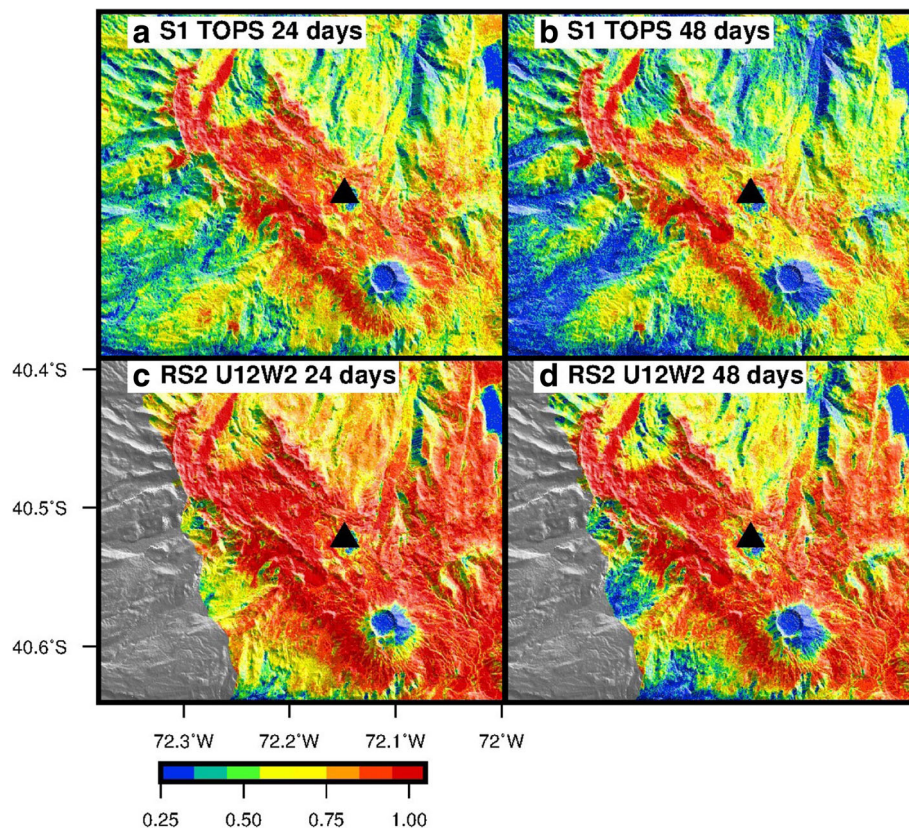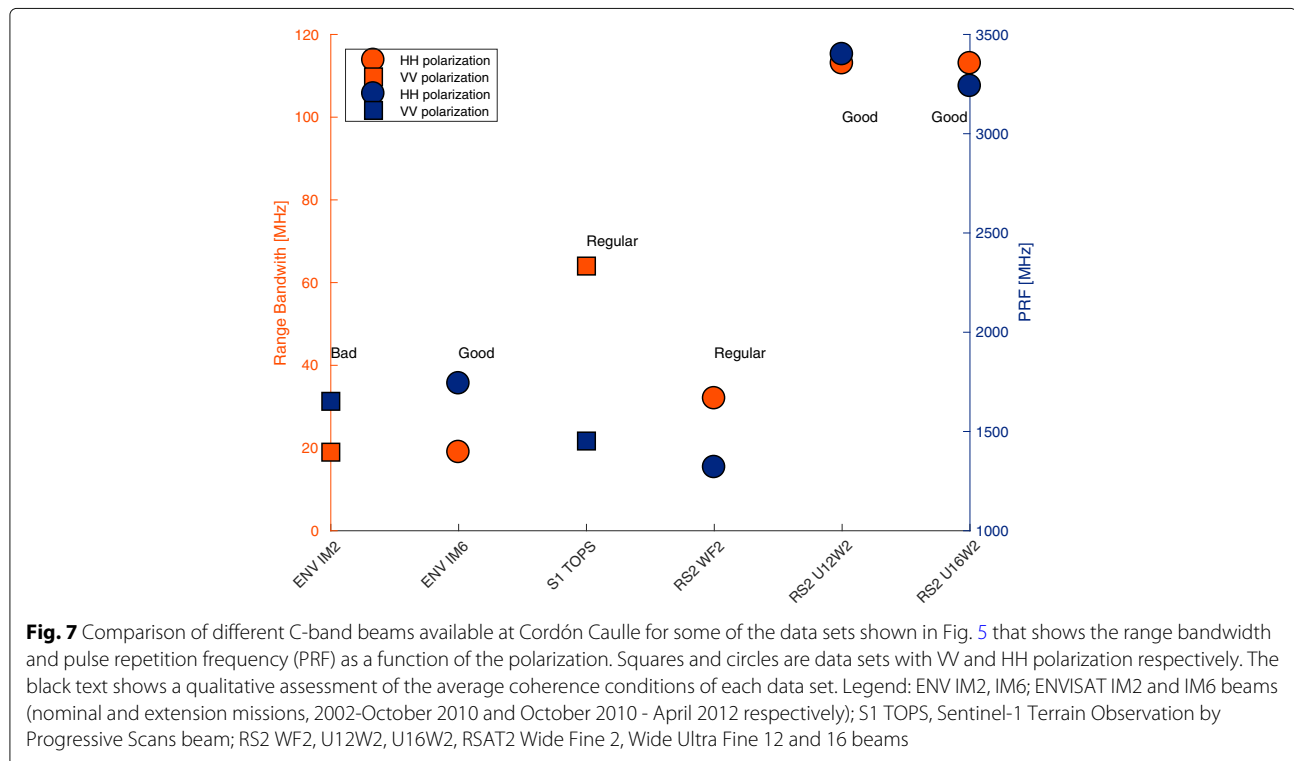
Pritchard *et al. Journal of Applied Volcanology* (2018) 7:5

Page 14 of 28

Fig. 6 Comparison of C-band average coherence in 24 and 48 days ascending interferograms (**a-c** and **b-d** respectively) of the Sentinel-1 Terrain Observation by Progressive Scans (TOPS) and RSAT2 Wide Ultra Fine 12 (U12W2) beams during January - May 2016 (austral summer - early fall) at Cordón Caulle volcano (Delgado et al. 2016). U12W2 beam SAR images were acquired three days after the TOPS ones. The average coherence of the U12W2 beam is higher than the TOPS beam (see Figs. 5 and 7)

observations are likely to be coherent, even if taken less frequently. However, the L-band observations suffer from extreme ionosphere problems spanning from Colombia to southern Chile (e.g. (Fournier et al. 2010; Morales-Rivera et al. 2016)). Quadratic ramps can be used to mitigate ionospheric signals for ALOS-2 stripmap data, but data from the ScanSAR beam requires a split-spectrum approach (e.g., (Liang and Fielding 2017)) because low order polynomials cannot capture the ionospheric complexity over such large swaths unless they are significantly cropped (e.g. (Euillades et al. 2017)).

Utility of X-band data for studying actively erupting volcanoes

X-band satellites such as CSK and TSX can provide higher spatial and temporal resolution data than other satellites, but X-band data are typically less coherent than C-band and L-band data (e.g., (Ebmeier et al. 2013b)). These satellites require more frequent data collects than the longer wavelength radars to maintain a coherent time series. Thus, analysis of X-band data is more resource intensive, both in terms of requiring large data quotas, as

well as computer and personnel time. However, the extra resources required for X-band data are not well characterized due to the small number of X-band datasets that have been analyzed to date, and so we describe the unique value of the X-band data at Masaya. Masaya has an ephemeral lava lake, occasional explosive eruptions and is persistently degassing (e.g., (Stix 2007)). An earlier study found long-term subsidence along the caldera ring fault using ALOS-1 data, but no deformation associated with magmatic processes close to the vent (Ebmeier et al. 2013b). For the LAPP, we focused on the transition between effusive and explosive behavior in May 2012 using a set of 40 CSK images spanning 8 months (Stephens et al. 2017). We find an alternating and unusual pattern of uplift and subsidence associated with the eruption – uplift in the month prior to the eruption, subsidence prior to the eruption, and back to uplift following the end of the eruption (Stephens et al. 2017). All the deformation occurs within 1.5 km of the vent and is consistent with a source within the upper 2 km of the magmatic plumbing system. The Masaya example demonstrates that detailed analysis of high spatial and temporal resolution datasets may reveal

Pritchard *et al. Journal of Applied Volcanology* (2018) 7:5

Page 15 of 28

Fig. 7 Comparison of different C-band beams available at Cordón Caulle for some of the data sets shown in Fig. 5 that shows the range bandwidth and pulse repetition frequency (PRF) as a function of the polarization. Squares and circles are data sets with VV and HH polarization respectively. The black text shows a qualitative assessment of the average coherence conditions of each data set. Legend: ENV IM2, IM6; ENVISAT IM2 and IM6 beams (nominal and extension missions, 2002-October 2010 and October 2010 - April 2012 respectively); S1 TOPS, Sentinel-1 Terrain Observation by Progressive Scans beam; RS2 WF2, U12W2, U16W2, RSAT2 Wide Fine 2, Wide Ultra Fine 12 and 16 beams

deformation associated with eruptions that is missed by large-scale InSAR surveys of short duration.

Associated SAR observations

In addition to interferograms to measure deformation described in the last sections, SAR satellites can also provide radar amplitude images and digital elevation models, which have the potential to be very useful to volcano observatories.

Radar amplitude

The amplitude component of a SAR image represents the power of the backscattered radar signal. The amplitude is a function of local slope relative to the SAR incidence angle, and the surface roughness on the length scale of the radar wavelength (e.g., (Wadge et al. 2011)). Changes in the observed radar amplitude can therefore provide information about areas that are affected by volcanic eruptions, even when the surface has changed enough to decorrelate the SAR phase.

At Cotopaxi Volcano, Ecuador, we observed changes in the summit glacier due to the minor explosive eruptions in August 2015 (Arnold et al. 2018). Comparing pre-eruptive and post eruptive images, we observe reduced amplitude within the summit crater in TSX, CSK (Fig. 8) and Sentinel-1a imagery (not shown). This amplitude decrease is likely due to deepening of the crater, which causes the crater floor to be in radar shadow and therefore receive no

illumination from the satellite. We also observe deposition of pyroclastic material on the inner crater flanks (Fig. 8b). CSK images show that relative to the pre-eruptive scene, the post eruptive scene has reduced amplitude on the glacier west of the summit, but increased amplitude further west on lower non glaciated areas (Fig. 8d and 8f). The prevailing wind direction at Cotopaxi blows from east to west, leaving the thickest tephra deposits to the west of the summit. At X-band wavelengths, the tephra deposits appear to be less rough than the glacial snow and ice (reduced amplitude) but more rough than the non-glaciated plateau surrounding Cotopaxi.

SAR amplitude images have been used at El Reventador, Ecuador, to map the spatial extent and temporal evolution of the lava flow between 2011 and 2016 (Arnold et al. 2017; Arnold et al. 2018). The width of the shadow cast by the steep sided lava flows was used to measure the thicknesses of the lava flow edges and therefore estimate flow volume and time-averaged lava extrusion rate. In addition to lava flows, we observe thinner deposits associated with pyroclastic density currents and can map their transition from erosive to depositional behaviour by observing the infilling of gullies. We also observe growth of the lava dome and formation and infilling of craters formed at the summit of the dome. El Reventador is a remote volcano situated in the Ecuadorian rainforest, and visual observations are frequently hindered by cloud cover. The all-weather imaging capability of SAR provides an ideal
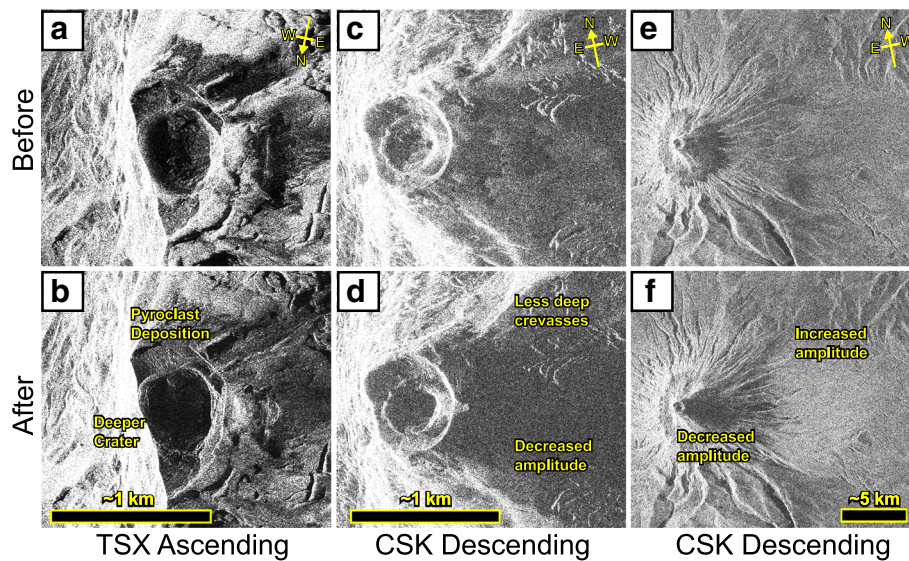
Pritchard *et al. Journal of Applied Volcanology*   (2018) 7:5

Page 16 of 28

Fig. 8 SAR amplitude images acquired before (top) and after (bottom) the August 2015 eruption of Cotopaxi Volcano, Ecuador. Images are in radar viewing geometry. **a** TSX spotlight image acquired 9 August 2015. **b** TSX spotlight image acquired 20 August 2015. **c** and **e** CSK stripmap image acquired 12 August 2015 at two different resolutions. **d** and **f** CSK stripmap image acquired 28 August 2015 shown zoomed in **d** and not in **f**

supplement to infrequent visual observations for volcano monitoring in these conditions.

Soufriere Hills Volcano, Montserrat is not currently erupting, but we used amplitude change detection methods to study Phase 5 of the eruption using 12 TSX images collected between Sept 2009 and February 2010 to test the applicability of this technique to future eruptions. In addition to the pyroclastic density currents (PDCs) detected by Wadge et al. (2011), we also detected amplitude changes associated with ashfall, lahars, and the weathering of recent eruptive products. The radar amplitude images are particularly useful for determining the spatial extent of the flows close to the dome, as the summit is often cloud-covered. In particular, since both PDCs and lahars are topographically controlled, knowing which direction the flows are following is key to hazard models. However, distinguishing between PDCs and lahars based on radar images alone is challenging, and we correlated our observations with those from the Montserrat Volcano Observatory. PDCs dominate in proximal valleys and typically display 'core-and-shell' pattern: the 'core' of the flow is formed by a rough surface surrounded by a shell of smoother deposits. Assuming pyroclastic flow deposits form through progressive aggradation (Branney and Kokelaar 1992), we interpret this rough core to be the initial deposits of dense material, with the shell representing more dilute aspects of the flow. In contrast, the lahar deposits exhibit a grading from smoother surfaces upstream to rougher surfaces downstream, following the characteristic of alluvial mudflow deposits (Lipman and Mullineaux 1981).

Sentinel-1 amplitude images spanning the 2015 eruption of Calbuco showed the formation of the new crater during eruptions on 22-23 April, which is especially clear in the ascending images, where the eastern rim of the new crater has a high amplitude (not shown). Eruptive deposits, including local ashfall northeast of the volcano, also caused amplitude changes and phase decorrelation in interferograms that spanned the eruption, most notably in topographic hollows downwind of the volcano.

High resolution digital elevation models

DEMs collected from space underpin a wide range of activities at volcano observatories, notably modeling the paths of hazardous flows (e.g., (Hubbard et al. 2007; Huggel et al. 2008)), but also estimating eruption flux and topographic corrections for geophysical datasets. The globally available DEMs, such as SRTM 1 and ASTER GDEM are too low resolution to be used for this purpose and where possible, observatories typically invest in airborne lidar or photogrammetric DEMs (e.g (Davila et al. 2007)). Both optical and radar satellites can also be used to repeatedly generate high-resolution DEMs (Section 1.2, e.g., (Poland 2014; Ebmeier et al. 2012)). It is possible to generate high resolution DEMs as often as every 11 days using CoSSCs from TanDEM-X bistatic SAR data (e.g., (Arnold et al. 2016)). DEMs generated by optical satellite stereo and tri-stereo images from the Pleiades system have been used at volcanoes in Latin America (e.g., (Castro et al. 2016 Richter et al. 2018)), but over some areas, clouds prevent clear data collection. For example, we had a three year standing request to collect Pleiades DEMs (tri-stereo

Pritchard *et al. Journal of Applied Volcanology* (2018) 7:5

Page 17 of 28

or stereo) over Chiles-Cerro Negro and Reventador, but after 100 attempts, no cloud free pairs could be collected.

Within the LAPP, we tested the utility of CoSSC-retrieved topography to measure the volume and distribution of volcanic products at fifteen target volcanoes: Santiaguito, Fuego and Pacaya, Guatemala; Arenal, Costa Rica; Soufriere Hills, Monserrat; Reventador, Ecuador; Ubinas, Perú; Nevado de Ruiz, Colombia; and Láscar, Copahue, Llaima, Vilarrica, Cordón Caulle, Chaitén and Hudson, all in Chile. Additional CoSSCs at Colima, Mexico were analyzed by (Kubanek et al. 2013). CoSSCs could have been useful at other volcanoes, but data were either not analyzed (like at Turrialba and Tungurahua) as part of the LAPP or not acquired, such at Calbuco after the VEI 4 2015 eruptions.

At Soufriere Hills, we generated DEMs from ALOS-1 L-band monostatic data in 2010–2011 and TanDEM-X X-band bistatic data in 2013 and compared them to earlier DEMs derived by aerial and ground-based photogrammetry surveys (Arnold et al. 2016). We observed cycles of dome building and collapse and the deposits of ash, pyroclastic flows and lahars with maximum elevation changes of 290 $\pm$ 10 m on the lava dome and 250 $\pm$ 10 m in valleys. In the case of Reventador, we generate 9 TanDEM-X DEMs which we complement with estimates of lava flow volumes from 32 RSAT2 amplitude images using the shadow method (Arnold et al. 2017). The resulting time-series enables us to investigate the temporal evolution of the effusion rate using physics-based models of the magmatic system (Arnold et al. 2017), and the behavior of basaltic-andestic lava flows. In both examples, areas of layover and shadow in the radar images introduce uncertainties, but at Montserrat, both the bistatic and monostatic InSAR methods provide a more complete quantification of deposits than the alternatives.

Topographic changes calculated from bistatic CoSSC data with respect to the SRTM DEM at several volcanoes in Latin America are shown in Fig. 9. Most of the topographic changes in Fig. 9 are due to the extrusion of lava flows and domes and to glacier retreat. The largest topographic changes result from the extrusion of a rhyolitic dome during the 2008-2009 Chaitén eruption (Fig. 9e, (Pallister et al. 2013b)) and the extrusion of a rhyodacitic lava flow as well as the intrusion of a very shallow laccolith during the 2011-2012 Cordón Caulle eruption (Fig. 9d, (Castro et al. 2016)). Topographic changes due to lava extrusion are also observed at Arenal (Fig. 9j, (Hofton et al. 2006)), Fuego (not shown), Santiaguito (Fig. 9l, (Ebmeier et al. 2012)) and for multiple eruptions at Pacaya (Fig. 9k, (Rose et al. 2013)). At Nevado del Ruiz, CoSSC analysis shows both glacier thinning and the growth of a small lava dome inside the volcano crater, although to properly image the latter signal we had to use the 12 m DLR World-DEM (Fig. 9h). At Ubinas we cannot image the growth of

a small lava dome (Fig. 9f, (Coppola et al. 2015)) inside the summit crater using SRTM as the reference topography. Signals observed at Villarrica and Llaima (Fig. 9a and b) are produced by glacier thinning and retreat, and during the 2015 and 2008-2009 eruptions, respectively (Delgado et al. 2017). At Hudson volcano we find more than 100 m of glacier thinning, including a topographic increase of 80 m in the ice filled caldera as well as in the 3 eruptive vents of its 2011 eruption (Fig. 9c, (Delgado et al. 2014b)). At Copahue volcano, we also find changes in the summit glaciers (Fig. 9i). Finally, at Láscar CoSSC analysis shows localized errors in the SRTM DEM (Fig. 9g), but no changes in the subsiding summit craters (e.g., (Richter et al. 2018)).

In summary, the CoSSC data are very useful at volcanoes where elevations are changing rapidly, which for Latin America, is at least 14 volcanoes during the LAPP. Although the spatial resolution of the CoSSCs allow construction of 2-4 m/pixel DEMs (even higher resolution for spotlight data), the minimum size of a topographic feature that can be detected depends on the resolution of the reference DEM. We have not assessed the minimum topographic change that can be detected by TanDEM-X, but it has been used to measure thicknesses of a few meters in basaltic flows elsewhere (Poland 2014), in agreement with theoretical uncertainties (Albino et al. 2015).

Feedback from volcano observatories

We received responses to a questionnaire regarding how the satellite observations from the LAPP were used and could be more effective (questions are shown in the Additional file 2) from eight volcano observatories (Table 4) in seven different countries. These volcano observatories are responsible for providing information about the possible hazards to their local and national governments. All satellite information should be conveyed to the authorities through the volcano observatories, and direct contacts of space agencies and external scientists with the media and authorities are highly discouraged since they could undermine the work of the observatories and reduce the effectiveness of the response (e.g., (Newhall et al. 1999)).

During the LAPP, all of the volcano observatories that completed the questionnaires used the satellite data with available ground observations to assess the possible hazard from a given volcano. When available, the satellite observations were discussed with the other types of data during regular staff meetings. The satellite data were not always available for decision support, either because they had not been acquired or processed in time. All observatories requested access to more frequent data made available in near real time. Because of the sub-optimal temporal sampling and timely data delivery, ground-based data
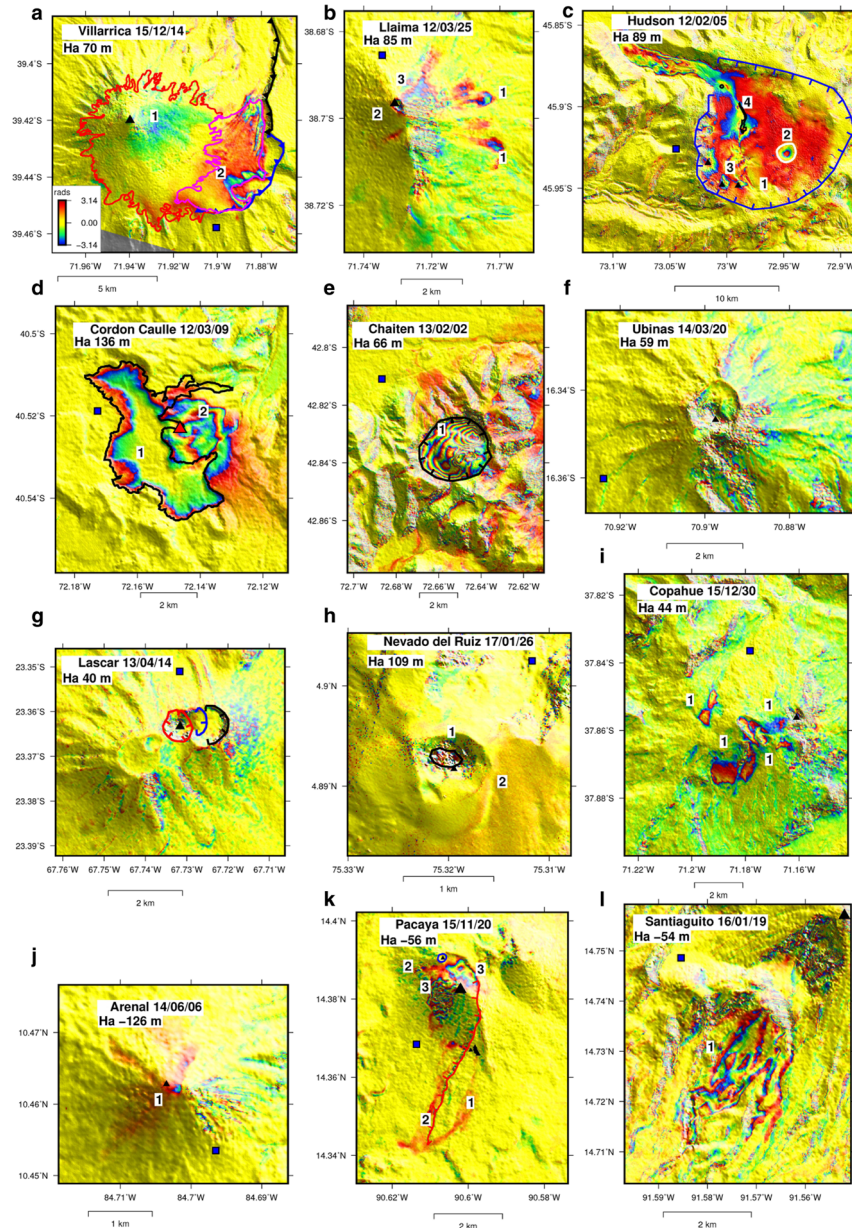
Pritchard *et al. Journal of Applied Volcanology*   (2018) 7:5

Page 18 of 28

Fig. 9 Topographic changes between February 2000 SRTM 1 arcsecond DEM (shaded relief) interpolated to 10 m and TanDEM-X acquisition (date shown). One color fringe equals the ambiguity height Ha shown in each subpanel which is a linear approximation for the actual topographic change that holds for values < 100 m. Blue squares are 10 by 10 pixels assumed to have zero topographic change. **a**. Villarrica: glacier thinning in the area of 2015 ash deposition (1) and glacier retreat (2). Volcano crater is black triangle, red and magenta lines are debris-free and debris-covered glacier (Rivera et al. 2015); blue and black lines are calderas 1-2 and 3 rims (Moreno and Clavero 2006); **b**. Llaima: debris-covered glaciers (1), summit change after the 2008-2009 eruptive cycle (2) and northern flank change (3) that is under investigation. Volcano crater is black triangle.; **c**. Hudson: thinning at glacier (A), uplift in an ice cauldron (2), the vents of the 2011 eruption (3) (Delgado et al. 2014b) and in areas of lahars (4). Black triangles are October 2011 eruptive vents, white line is an ice filled cauldron, black lines are lahars observed in early 2011 and blue line is caldera rim (Delgado et al. 2014b).; **d**. Cordón Caulle: new rhyolitic lava flow (1), intrusion of shallow laccolith (2) (Castro et al. 2016). Black line is contour of the 2011-2012 lava flow one year after the end of the eruption, red triangle is eruptive vent (Delgado et al. 2016).; **e**. Chaitén: new rhyolitic lava dome (1) (Pallister et al. 2013b). Black line is caldera rim.; **f**., **g**. no changes at Láscar and Ubinas, but SRTM errors. Black triangle is eruptive vent. Red, blue and black lines are crater A, B and C at Láscar (de Zeeuw-van Dalfsen et al. 2014).; **h**. Nevado del Ruiz (used the 12 m DLR WorldDEM instead of SRTM): glacier thinning (1) and growth of a small dome (2). Black triangle is eruptive vents.; **i**. Copahue: glacier changes (1). Black triangle is eruptive vents.; **j**. Arenal: new lava flows (1), Black triangle is eruptive vents.; **k**. Pacaya: lava flows extruded in May 2010 (1), 2014 (2), 2004-2008 (3) (Wnuk and Wauthier 2017) black triangles are eruptive vents and red line is a collapse scarp (Wnuk and Wauthier 2017); and **l**. Santiaguito: new lava flows and domes (1). Black triangle is eruptive vents

Pritchard *et al. Journal of Applied Volcanology*   (2018) 7:5

Page 19 of 28

Table 4 Volcano observatories contacted during the LAPP

Volcano Observatory: Country
Centro Nacional de Prevención de Desastres (CENAPRED): Mexico
[a]Instituto Nacional de Sismologia, Vulcanología, Meteorología e Hidrologia (INSIVUMEH): Guatemala
Servicio Nacional de Estudios Territoriales (SNET): El Salvador
[a]Instituto Nicaragüense de Estudios Territoriales (INETER): Nicaragua
[a]Observatorio Vulcanológico y Sismológico de Costa Rica (OVSICORI): Costa Rica
Montserrat Volcano Observatory (MVO): Montserrat
Seismic Research Centre, University of the West Indies, Trinidad and Tobago (SRC_UWI): English-speaking Eastern Caribbean
[a]Observatorio Vulcanológico y Sismológico de Pasto (OVSP), Servicio Geológico Colombiano (SGC): Colombia
[a]Observatorio Vulcanológico y Sismológico de Manizales (OVSM), Servicio Geológico Colombiano (SGC): Colombia
[a]Instituto Geofisico-Escuela Politecnica Nacional (IG-EPN): Ecuador
[a]Observatorio Vulcanológico del Sur del Instituto Geofisico del Perú (IGP-OVS) & Observatorio Vulcanológico del Instituto Geológico, Minero y Metalúrgico (OVI-INGEMMET): Perú
Observatorio San Calixto, Bolivia
[a]Observatorio Vulcanológico de los Andes del Sur (OVDAS), Servicio Nacional de Geología y Minería (SERNAGEOMIN): Chile
Observatorio Argentino de Vigilancia Volcánica del Servicio Geológico Minero Argentino (SegemAR-OAVV): Argentina

[a] Indicates those that completed questionnaires for the LAPP

(seismicity, geochemistry, GPS) are used more regularly to define warning levels.

For example, in Perú, the LAPP did not have the personnel to process interferograms routinely for all volcanoes. We were either monitoring background activity annually or operating in a reactive mode, responding to episodes of unrest. There were about a dozen of these requests for the 4 volcanoes where unrest was detected on the ground (see Table 3: Ubinas, Sabancaya, Ticsani, El Misti). The volcano observatories write weekly reports and would include satellite observations more often if data were available.

We summarize here a few comments from the questionnaires. The volcano observatories use information from satellite data in their communications with local communities and decision-makers, but the data themselves are not usually included. The volcano observatories receive the images (for example, interferograms) which meets most of their needs, but written scientific interpretations of the images are considered helpful. Additional model-based information (when available) like parameters of best-fitting source models are useful for comparison with other inferences. Some participants in the pilot identified two groups of products that are both of value to the observatories – interferograms produced for hazard assessment (i.e., produced rapidly, including null results of immediate value for understanding if there is a large change in the system or not) and interferograms and time series produced for science that take longer time and allow the detection of smaller amplitude signals.

In terms of capacity building, short courses and visits by InSAR experts to the observatory or observatory staff to an InSAR processing center are considered useful for interpreting the data – both types of activities occurred during the LAPP. We have recommendations on how to improve uptake by volcano observatories in the "Discussion" section. An important outcome of the questionnaires is that each volcano observatory is unique in the number of people and amount of resources – thus, while some would like to set up capability to have a staff member take an active role in processing InSAR data, other observatories do not have resources for this and will rely on external partners to process data and provide interpretations.

Discussion

Recommendations for global subaerial satellite volcano observing system

The LAPP has tested the concept of a regional scale volcano monitoring system. In doing so, we have gained insights into the requirements for and challenges of an operational global volcano monitoring system based on satellite observations as envisioned in the Santorini report in 2012. We note that the Santorini report objectives are not yet achievable without some further international coordination. Using our experience from the LAPP, we discuss below seven practical principles that the SAR component of a global satellite volcano monitoring system should consider. While these principles may be self-evident to many in the SAR community, they need to be communicated to the space agencies and volcano observatories. We first list the principles and then discuss each in more detail.

1 The monitoring system must involve multiple space agencies and satellite platforms, to get nearly daily

Pritchard *et al. Journal of Applied Volcanology*   (2018) 7:5

Page 20 of 28

coverage and to provide regularly updated high resolution topographic maps.

2 Data quotas should be assigned for a) systematic background observations using the appropriate observing mode for each volcano (spatial resolution, polarization, etc.), b) case studies requiring very high temporal resolution datasets and c) flexible response to unrest and eruption.

3 A systematic background mission using ascending and descending passes should take into account both the level of activity at each volcano and the temporal and spatial baselines required to form coherent interferograms and observe deformation transients.

4 Acquisition plans need to be flexible to accommodate changes in activity, evolving methods, and improved understanding of which observation modes are and are not useful at each volcano.

5 Near real-time data access is vital for decision making, requiring frequent overpasses, rapid tasking and short data latency.

6 Dedicated support for coordination between space agencies, scientists and volcano observatories to provide the best operational response and avoid conflicting requests for the satellite tasking or interpretations of satellite observations.

7 Long-term sustainability is key to building and maintaining relationships with observatories and decision-makers. Research projects and students can provide support, but stable resources should be ensured.

Optimising acquisitions from a multi-platform virtual constellation

Radar satellites operate at a range of different frequencies and polarisations, repeat intervals and resolutions. Similarly, volcanoes have different characteristics. The goal of a virtual constellation is to assign the appropriate satellite(s) and mode(s) for each volcano. At the start of the LAPP, we planned the type of data needed at each volcano, but it soon became apparent that the plan needed to be reviewed on a regular basis to take into account changes in volcanic activity and satellite availability.

The spatial resolution required depends on the type of volcano and activity. High spatial resolution (better than 1 m/pixel) is required at volcanoes where activity is concentrated in a small area, such as the summit crater of a stratovolcano, or where the volcanic system is open, and deformation is associated with shallow conduit processes (like Colima volcano, Mexico, and Masaya volcano, Nicaragua, (Salzer et al. 2014; Stephens et al. 2017)). In contrast, large calderas, or deep magma systems require large footprints to capture the broad deformation pattern (like Nevado del Ruiz, Colombia and Villarica, Chile, (Lundgren et al. 2015; Delgado et al. 2017)). More broadly,

there are many examples (in Latin America: Cordón de Puntas Negras, Lazufre, recent Nevado de Ruiz deformation) where deformation is centered 10-30 km from the volcano edifice, and imaging the edifice alone in a high resolution mode could miss the deformation signal (e.g., (Delgado et al. 2017; Ebmeier et al. 2018)).

Volcanic processes operate over a range of timescales, some of which are too short to ever be captured by polar-orbiting satellites. However, short-lived deformation pulses, such as the pre-eruptive deformation at Llaima, Chile (caught by chance by ALOS-1, (Delgado et al. 2017; Chen 2017)) and Masaya, Nicaragua (Stephens et al. 2017) can be measured using sub-weekly overpasses provided by satellite constellations such as CSK and Sentinel-1 if a large data quota is available.

The coherence of interferograms is limited by the radar wavelength and the temporal and geometric baseline between acquisitions, and depends on surface characteristics, particularly vegetation cover. The current 12-24 day repeat interval for Sentinel-1 is not sufficient to maintain coherence in many volcanic areas in Latin America, specifically southern Chile and Central America (Additional file 2: Figure S6). The LAPP examples illustrate the need for systematic studies of atmospheric artifacts and interferometric coherence at different wavelengths (e.g., (Parker et al. 2015; Ebmeier et al. 2013b; Delgado et al. 2017)), to tailor the acquisition plans. For Sentinel-1, this might mean 24 day repeats in areas of good coherence, but more frequent acquisitions in other areas. ALOS-2, which operates at L-band and high bandwidth HH polarized RSAT2 can be used to supplement Sentinel-1 for areas that are extremely vegetated, such as Central America and the southern Andes.

Background mission

Background observations are critical to develop a complete archive of both positive and null results of deformation across a spectrum of volcano types and tectonic settings – avoiding the problem that information about unrest that does not lead to eruption (so called failed eruptions) is often not published in the literature (e.g., (Moran et al. 2011; Biggs et al. 2014)). During the LAPP, tasking conflicts occurred between groups who were requesting different beam modes with different priority levels. In the worst case, this interrupted a long-term time series at a crucial phase of unrest. For RSAT2, although the acquisitions are frequent, they not systematic, with irregular acquisitions using different modes and resolutions. This can be an advantage, for example, the randomness in acquisitions allowed the Mauna Kea pit crater to be imaged when it is not normally visible (observed by co-author Mike Poland), but can also lead to a lack of consistency in results and challenges in planning for upcoming acquisitions.

Pritchard *et al. Journal of Applied Volcanology* (2018) 7:5

Page 21 of 28

One way to avoid tasking conflicts is to ensure a background observation strategy defined by a steering group of users as already being done by ESA and ASI. A more effective acquisition strategy to provide the most useful data for volcano disaster risk reduction could be defined at the inter-agency level. Such a background mission would ensure that there is a suitable archive of data for each volcano, enable detection of unrest at unmonitored volcanoes, and avoid tasking conflicts.

Deformation captured with infrequent acquisitions can be retrospectively studied with higher resolution provided there is a background mission. For example, Sentinel-1 was able to capture deformation associated with the reappearance of the lava lake at the Santiago crater pit (2015-present) at Masaya, Nicaragua, and motivated the LAPP to order CSK data.

Background missions should include data collection during both ascending and descending satellite orbits. There are several examples in Latin America where using only one or the other has meant that the deformation was not detected (e.g., Arenal flank displacements are hard to detect in ascending data, (Fournier et al. 2010; Ebmeier et al. 2013a)) or the true complexity of the source of the deformation was only revealed when both data were

available (e.g., (Wicks et al. 2011; Jay et al. 2014; Delgado et al. 2017; Lundgren et al. 2017; Nikkhoo et al. 2017)).

Data quotas and access

Particularly in the tropics, time series methods are required to mitigate against atmospheric artifacts and poor coherence (e.g., (Stephens et al. 2017)). For CSK, many of the short temporal baseline image pairs have large perpendicular baselines making them incoherent (Fig. 10). Compounding the problem is the fact that baselines are not defined in the acquisition catalogue requiring the processing of all images to find the coherent results. Depending on the conditions, many hundreds of images may be required to study just a few volcanoes (Figs. 10, 11). Thus even though the quotas allocated to the LAPP were very generous, they were not sufficient for all detailed studies requested by the volcano observatories.

Near real-time data access is vital for including InSAR observations in decision-making processes during volcanic crises. By using a virtual constellation, there is often a planned acquisition within a day or two of receiving a request from an observatory, and if not, an acquisition can be requested on an upcoming overpass. For instance, the repeat pass of CSK is as little as 12 h when all 4 satellites and pass directions are taken into account.
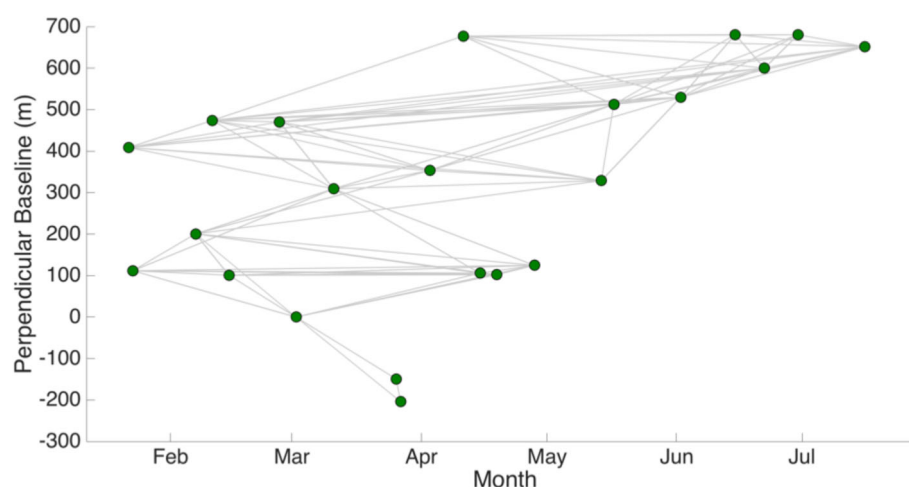
Fig. 10 CSK data acquisitions over time at Villarrica showing data analyzed (blue circles) the timing of the 2015 eruption (red line), and the perpendicular baseline. Blue circles that are connected were the only small baseline interferograms that were coherent in the vegetated areas that surround the volcano for postings of 30 m. Because the subsets do not overlap in time and in the absence of clear deformation signals it is very difficult to properly tie them for a time series inversion

Pritchard *et al. Journal of Applied Volcanology* (2018) 7:5

Page 22 of 28

Fig. 11 Twenty two CSK data acquisitions over the Masaya region showing data analyzed (green circles) spanning the 2012 explosive eruption sequence and their perpendicular baselines plotted as a function of date 2 March 2012. Connected green circles indicate the 54 interferograms used for time-series analysis with a perpendicular baseline of less than 230 m (Stephens et al. 2017)

Within the LAPP, the most significant delays were associated with data latency, rather than limitations of satellite acquisitions. In particular, TSX acqusitions typically have a latency of 4-5 days, which meant that despite an ongoing timeseries of TSX data, we relied on other satellites to provide information during Chiles-Cerro Negro crisis (Ebmeier et al. 2016). The Sentinel-1 ground segment was still in its setup phase during the LAPP, but data access is improving with time.

Coordination and communication
A significant challenge to the LAPP was coordination, and dedicated personnel would be needed to extend the efforts of the pilot into a long-term monitoring system. Systematic monitoring of volcanoes in Latin America will require a dedicated effort by a team of scientists. The LAPP relied heavily on case studies produced by PhD students, but they cannot sustain demands of operational monitoring. Nor are short-term research projects suitable for long-term sustainability. Indeed previous attempts to set up satellite-based monitoring have developed promising software solutions, but are no longer maintained (e.g., (Tait and Ferrucci 2013))

Limitations of the LAPP
The 3-year duration of the LAPP (extended to 4 years with archive data) did not cover all of the types of volcanic activity that could occur. The short duration of any satellite observations will not sample the lifecycle of any individual volcano and we must rely on the ergodic hypothesis – that we can substitute sampling the entire range of behaviours in time by instead sampling in space. But the four year time period was clearly too short to characterize volcanic activity and its hazard – for

example, as far as we can tell, during the LAPP, there were no deaths attributed to volcanic activity. In contrast, volcanic activity in the region during the 20th century caused about 62,345 deaths (623/year), but with 88% from just two eruptions – 1902 at Mt. Pelee (Martinique) and 1985 Nevado de Ruiz, Colombia (Cred 2017). The CRED database spans 1900-2016 and includes about 85 unique volcanic disasters in Latin America (0.73/year or about 3 expected during the LAPP time period) that meet their criteria (more than 10 deaths or 100 people affected, declaration of a state of emergency, or request for international assistance). In fact, eight events occurred during the LAPP that are recorded in Cred (2017) – all for eruptions between 2013-2015: Villarrica and Calbuco, Chile (with Calbuco listed in the database as separate entries for Chile and Argentina); Sabancaya and Ubinas, Perú (grouped together); San Miguel, El Salvador; Cotopaxi and Tungurahua, Ecuador; and Turrialba, Costa Rica, that caused significant damage and collectively affected > 1 million people (with 80% affected by Cotopaxi). This shows the impact of single, rare events and shows the need for a longer time series of observations.

Recommendations to improve uptake of InSAR data by volcano observatories
Based on the interaction of the LAPP with eight volcano observatories over several years and completed questionnaires, we offer the following suggestions on how to improve uptake of InSAR data at the volcano observatories in Latin America:

1 Training in data processing and interpretation.
   As part of the LAPP and related activities, we have been involved in short courses to train observatory

Pritchard *et al. Journal of Applied Volcanology*   (2018) 7:5

Page 23 of 28

staff in Colombia, Ecuador, Chile, Costa Rica and Guatemala as well as training courses in the USA and UK that included personnel from Latin America. Reviews from these courses indicate that they are valuable to the volcano observatory staff and additional training courses in country have been requested. One of the observatories seeks to establish their own on-site expertise to analyze the InSAR data – in this case, some graduate-level training is necessary, either full degrees or a few months visit. In Ecuador, some InSAR processing has already begun, although the staff member building the experience is temporary. OVSICORI in Costa Rica has hired a University of Bristol PhD graduate, to their geodesy section, and although he has experience in InSAR processing and analysis, his time is mostly taken up with ground-based monitoring. Observatories commented that receiving processed interferograms is valuable; even when they process the data at the observatory, having a second opinion on the interpretation is appreciated, when it comes from a trusted source.

2 Access to software, computers, and satellite imagery. Computing costs are decreasing globally, but commercial InSAR software is still too expensive for many Latin American observatories. Open-source software is preferred (SNAP, GMTSAR, ISCE, DORIS). Of course, open source software has limitations – for example, there is not always sufficient user support and the software is not always capable of dealing with new data (for example, a version of ISCE that could stitch Sentinel-1 swaths was released 3 years after the launch, and the zero-doppler Single Look Complex data files are not correctly processed). Further, access to datasets is challenging because of the number of different satellite systems (each having a different website and data system), and large file sizes.

3 Data Distribution
   If data products are created by external partners, there are several potential ways they could be distributed to volcano observatories. In some cases, a simple image (jpeg) is of use, but observatories appreciate georeferenced images in Google Earth or ArcGIS. As automated systems are developed for processing data and creating alerts (e.g., (Hua et al. 2013; Spaans et al. 2017)), several possible strategies could be established: 1) Use the existing Smithsonian weekly reports but add satellite unrest detections, make them available in foreign languages, and allow users to select to only get updates for certain volcanoes; 2) create automatic alert subscriptions, similar to those of Pavolonis et al. (2016) where the user can specify targeted volcanoes and receive an

email as soon as there is a detection. Such alerts are currently used for targeting additional satellite acquisitions for a limited number of volcanoes (Ramsey 2016). 3) Websites associated with dedicated processing systems, such as the LicSAR system being developed by the NERC-COMET group (http://comet.nerc.ac.uk/COMET-LiCS-portal/), which aims to produce Sentinel-1 interferograms for every volcano in the world. For archived observations, WOVOdat and the Smithsonian Institution store some raw data, but at the moment this is only in the form of jpegs, not the digital data that could be used in modeling.

4 Conflicting Advice.
   For products provided by external partners, one concern is conflicting interpretations. In recent years, volcano observatories have received interferograms that some people interpreted as ground deformation, but others thought was atmospheric noise. In other cases, deformation was attributed to a dyke, a sill or fault slip. Observatories request that uncertainties are included in any products they are sent – specifically whether a given signal is likely to be real deformation or an atmospheric or ionospheric effect. There are ethical and possibly legal implications in providing information to an end-user who has not enough expertise to assess the quality of the product, but still is the only one liable for the losses if any arise from incorrect information or even misuse (e.g., (Aspinall 2011)). When multiple groups are interpreting interferograms and communicating with the volcano observatory that does not have InSAR expertise, some procedures should be established so that the external groups can work together to provide one consensus interpretation or the range of interpretations available considering the ethical and legal implications (e.g., (Aspinall 2011; Bretton et al. 2015)). Further, those providing satellite data to observatories have an obligation to ensure there is capacity at the observatory, if not to process the data, at least with the interpretation of satellite products.

Conclusions

Most of the goals of the LAPP outlined in "The CEOS volcano pilot project: motivation and implementation" section were achieved:

1 *Identification of volcanoes that are in a state of unrest:* The LAPP discovered unrest that was not detected by ground sensors (e.g., Córdon Caulle, Chile), and confirmed or complemented ground arrays in other areas. Due to limits in data and personnel availability, the LAPP was not able to monitor all volcanoes in Latin America as frequently

Pritchard *et al. Journal of Applied Volcanology* (2018) 7:5

Page 24 of 28

as desired (i.e., quarterly for all 319 volcanoes or weekly at 63 "active" volcanoes), but concentrated on 42 "active" volcanoes with background observations at > 200 others.

2 *Comprehensive tracking of unrest and eruptive activity:* The LAPP motivated the end-users at volcano observatories to do a few things differently than they would have done without satellite data – such as install instruments in areas that were discovered by the LAPP to be deforming, support situational awareness during volcanic crises, contribute to the interpretation that a large eruption was not imminent (and thus helped to lower or keep an alert level low), and to show failures in ground sensors. It is impossible to put an economic impact on the value of satellite observations as part of the LAPP. As far as we know, no lives were lost during the LAPP, but about 1 million people were affected by eight eruptions noted by Cred (2017) during the four year time period of the LAPP. Satellite data contributed to the volcano observatory's decision-making about alert levels, sensor deployments, and the reliability of sensors for five of those eight eruptions (Calbuco, Villaricca, Sabancaya, Cotopaxi, Tungurahua).

3 *Validation of EO-based methodology for improved monitoring:* It is clear that a virtual constellation added value – some unrest could only be detected or constrained by certain satellites (Table 2).

4 *Improved EO-based monitoring of key parameters for volcanoes that are about to erupt, are erupting, or have just erupted:* Satellite observations allowed lava flows to be monitored at remote Reventador, Ecuador, and provided the only ground deformation data and constraints on magma resrvoirs during the 2014 eruptions at Wolf, Ecuador and Pacaya, Guatemala.

5 *Capacity-building:* The LAPP provided training in SAR/InSAR interpretation and increased the amount of SAR data being used in decision-making at volcano observatories. But there is more work to be done to make the data available in a timely manner to allow for more routine use as well as to reach out to every single volcano observatory in the region.

To improve upon the work of the LAPP, the critical needs are continued access to restricted SAR datasets and more frequent data provided at lower latency. We are currently limited in the amount of data being acquired, but also there is sometimes a delay between when data are tasked or acquired and when it can be delivered because personnel are limited and there are other pressing needs. The situation will improve with the routine 12 or 24 day background mission

from Sentinel-1, but there are still gaps in Sentinel-1 coverage.

We think that the work of the LAPP should continue through a coordinated project between volcano observatories, space agencies, and international scientists. It is our view that the primary hurdles for continuing the volcano disaster risk reduction work of the pilot are the definition of dedicated teams to accomplish the work (at the observatories and externally) and the commitment from space agencies (and their partners) to provide relevant data. Central to the team aproach is capacity building and should include the training of students from the countries that need the capability to process and interpret remote sensing data, instead of solely short courses and isolated outreach efforts. It is also clear to us that there is not a one-size fits all approach to linking volcano observatories and satellite data – at one extreme, some observatories would like raw data to process themselves to compare with results from external partners while at the other extreme the observatories do not have staff to process raw data and so would like interpreted products provided. It should also be recognized that there are some remote volcanoes that are not being actively monitored by any observatory. An approach that identifies the needs of different volcano observatories and is able to address all of these different capabilities is needed.

Additional file

Pritchard *et al. Journal of Applied Volcanology* (2018) 7:5

Page 25 of 28

Publisher's Note

Author details
[1]Department of Earth and Atmospheric Sciences, Cornell University, 112 Hollister Drive, 14850 Ithaca, NY, USA. [2]School of Earth Sciences, University of Bristol, Queens Road, BS8 1RJ Bristol, UK. [3]Department of Geosciences and Institute for CyberScience, The Pennsylvania State University, 311 Deike Building, 16802-2714 University Park, PA, USA. [4]Institute for Electromagnetic Sensing of Environment (IREA), National Research Council (CNR), via Diocleziano, 328, 80124 Napoli, Italy. [5]School of Earth and Environment, University of Leeds, LS2 9JT Leeds, UK. [6]Department of Earth and Space Sciences, University of Washington, 98195-1310 Seattle, WA, USA. [7]Rosenstiel School of Marine and Atmospheric Science, University of Miami, 4600 Rickenbacker Cswy, 33136 Miami, FL, USA. [8]Instituto Geofisico de la Universidad Nacional de San Agustín, Arequipa, Perú. [9]Instituto Geofisico, Escuela Politecnica Nacional, Casilla 1701-2759, Quito, Ecuador. [10]Observatorio Vulcanológico del Sur, Instituto Geofísico del Perú, Urb. La Marina B-19„ Arequipa, Perú. [11]Servicio Nacional de Geología y Minería (SERNAGEOMIN), Av. Santa María 0104, Santiago, Chile. [12]U.S. Geological Survey - Cascades Volcano Observatory, 1300 SE Cardinal Ct., Suite 100, 98683-9589 Vancouver, WA, USA. [13]Agenzia Spaziale Italiana (ASI), Viale Liegi, 26, 00198, Roma, Italy.

References

Albino F, Smets B, d'Oreye N, Kervyn F. High-resolution TanDEM-X DEM: An accurate method to estimate lava flow volumes at Nyamulagira Volcano (D. R. Congo). Journal of Geophysical Research. 2015;120.4189–207.

Anderson KR, Poland MP, Johnson JH, Miklius A. Episodic deflation-inflation events at Kīlauea Volcano and implications for the shallow magma system. Hawaiian Volcanoes: From Source to Surface. 2015;208.229.

Arnold DWD, Biggs J, Wadge G, Mothes P. Using satellite radar amplitude imaging for monitoring syn-eruptive changes in surface morphology at an ice-capped stratovolcano. Remote sensing of Environment. 2018;122. In press.

Arnold D, Biggs J, Wadge G, Ebmeier S, Odbert H, Poland MP. Dome growth, collapse, and valley fill at Soufrière Hills Volcano, Montserrat, from 1995 to 2013: Contributions from satellite radar measurements of topographic change. Geosphere. 2016;12(4):1300–15.

Arnold D, Biggs J, Anderson K, Vallejo Vargas S, Wadge G, Ebmeier S, Naranjo M, Mothes P. Decaying lava extrusion rate at El Reventador Volcano, Ecuador, measured using high-resolution satellite radar. J Geophys Res Solid Earth. 2017;122.9966–88. https://doi.org/10.1002/2017JB014580.

Aspinall W. Check your legal position before advising others. Nat News. 2011;477(7364):251.

Bally P. Scientific and Technical Memorandum of the International Forum on Satellite EO and Geohazards, 21–23 May 2012. European Space Agency Publication STM-282; 2012, p. 170. https://doi.org/10.5270/esa-geo-hzrd-2012.

Bernard B, Ramon P, Wright H, Guevara A, Hidalgo S, Pacheco S, Narvaez D, Vasconez F. Preliminary results on the 2015 eruption of Wolf volcano, Isabela Island, Galápagos: Chronology, dispersion of the volcanic products, and insight into the eruptive dynamics (abstract V31B-3022). In: AGU Fall Meeting Abstracts. San Francisco: American Geophysical Union; 2015.

Biggs J, Pritchard M. Global volcano monitoring: What does it mean when volcanoes deform?. Elements. 2017;13. https://doi.org/10.2113/gselements.13.1.17.

Biggs J, Mothes P, Ruiz M, Amelung F, Dixon TH, Baker S, Hong S-H. Stratovolcano growth by co-eruptive intrusion: The 2008 eruption of Tungurahua Ecuador. Geophys Res Lett. 2010;37(21). https://doi.org/10.1029/2010GL044942.

Biggs J, Ebmeier S, Aspinall W, Lu Z, Pritchard M, Sparks R, Mather T. Global link between deformation and volcanic eruption quantified by satellite imagery. Nat Commun. 2014;5(3471). https://doi.org/10.1038/ncomms4471.

Branney MJ, Kokelaar P. A reappraisal of ignimbrite emplacement: progressive aggradation and changes from particulate to non-particulate flow during emplacement of high-grade ignimbrite. Bull Volcanol. 1992;54(6):504–20.

Bretton RJ, Gottsmann J, Aspinall WP, Christie R. Implications of legal scrutiny processes (including the L'Aquila trial and other recent court cases) for future volcanic risk governance. J Appl Volcanol. 2015;4(1):18.

Brown S, Loughlin S, Sparks R, Vye-Brown C. Global volcanic hazards and risk: Technical background paper for the global assessment report on disaster risk reduction 2015. 2015a. http://www.preventionweb.net/english/hyogo/gar/2015/en/bgdocs/GVM,%20201%4b.pdf. Accessed 8 Aug 2017.

Brown S, Sparks R, Mee K, Vye-Brown C, Ilyinskaya E, Jenkins S, Loughlin S. Regional and country profiles of volcanic hazard and risk; 2015b. http://www.preventionweb.net/english/hyogo/gar/2015/en/bgdocs/risk-sectio%n/GVMd.%20Global%20Volcanic%20Hazards%20and%20Risk%20Country%20volcanic%%20hazard%20and%20risk%20profiles..pdf. Accessed 8 Aug 2017.

Bürgmann R, Rosen PA, Fielding EJ. Synthetic aperture radar interferometry to measure Earth's surface topography and its deformation. Ann Rev Earth Planet Sci. 2000;28.169–209.

Castro JM, Cordonnier B, Schipper CI, Tuffen H, Baumann TS, Feisel Y. Rapid laccolith intrusion driven by explosive volcanic eruption. Nat Commun. 2016;7.10–103813585.

Chaussard E, Amelung F, Aoki Y. Characterization of open and closed volcanic systems in Indonesia and Mexico using InSAR time series. J Geophys Res Solid Earth. 2013;118(8):3957–69.

Chen Y. Analyse InSAR des déformation de volcans actifs: le Piton de la Fournaise (Réunion) et le Llaima (Chili). PhD thesis, PhD Thesis, Université Toulouse III; 2017. https://tel.archives-ouvertes.fr/tel-01501284/file/THESE_CHEN.pdf. Accessed 9 June 2018.

Coppola D, Macedo O, Ramos D, Finizola A, Delle Donne D, del Carpio J, White R, McCausland W, Centeno R, Rivera M, Apaza F, Ccallata B, Chilo W, Cigolini C, Laiolo M, Lazarte I, Machaca R, Masias P, Ortega M, Puma N, Taipe E. Magma extrusion during the Ubinas 2013-2014 eruptive crisis based on satellite thermal imaging (MIROVA) and ground-based monitoring. J Volcanol Geotherm Res. 2015;302.199–210.

Cred E. The OFDA/CRED International Disaster Database; 2017. http://www.emdat.be/disaster_list/index.html. Accessed 8 Aug 2017.

Davila N, Capra L, Gavilanes-Ruiz J, Varley N, Norini G, Vazquez AG. Recent lahars at Volcán de Colima (Mexico): Drainage variation and spectral classification. J Volcanol Geotherm Res. 2007;165(3):127–41.

de Zeeuw-van Dalfsen E, Richter N, González G, Walter TR. Geomorphology and structural development of the nested summit crater of láscar volcano studied with terrestrial laser scanner data and analogue modelling. J Volcanol Geotherm Res. 2014;329.1–12.

Dehn J, Dean KG, Engle K, Izbekov P. Thermal precursors in satellite images of the 1999 eruption of Shishaldin Volcano. Bull Volcanol. 2002;64(8): 525–34.

Delgado F, Pritchard M, Biggs J, Arnold D. Utility of regional satellite volcano deformation monitoring in Latin America: The CEOS pilot project (abstract V41C-4830). In: AGU Fall Meeting Abstracts. San Francisco: American Geophysical Union; 2014a. p. 4830.

Delgado F, Pritchard M, Lohman R, Naranjo JA. The 2011 Hudson volcano eruption (southern Andes, Chile): Pre-eruptive inflation and hotspots

Pritchard *et al. Journal of Applied Volcanology*   (2018) 7:5

Page 26 of 28

observed with insar and thermal imagery. Bull Volcanol. 2014b;76(5): 815.

Delgado F, Pritchard ME, Basualto D, Lazo J, Córdova L, Lara LE. Rapid reinflation following the 2011–2012 rhyodacite eruption at Cordón Caulle volcano (southern Andes) imaged by InSAR: Evidence for magma reservoir refill. Geophys Res Lett. 2016;43(18):9552–62.

Delgado F, Pritchard ME, Ebmeier S, González P, Lara L. Recent unrest (2002–2015) imaged by space geodesy at the highest risk Chilean volcanoes: Villarrica, Llaima, and Calbuco (Southern Andes). J Volcanol Geotherm Res; 2017. https://doi.org/10.1016/j.jvolgeores.2017.05.020.

Ebmeier SK, Andrews BJ, Araya MC, Arnold DWD, Biggs J, Cooper C, Cottrell E, Furtney M, Hickey J, Jay J, Lloyd R, Parker AL, Pritchard ME, Robertson E, Venzke E, Williamson JL. Synthesis of global satellite observations of magmatic and volcanic deformation: implications for volcano monitoring & the lateral extent of magmatic domains. J Appl Volcanol. 2018;7. https://doi.org/10.1186/s13617-018-0071-3.

Ebmeier S, Biggs J, Mather T, Elliott J, Wadge G, Amelung F. Measuring large topographic change with InSAR: Lava thicknesses, extrusion rate and subsidence rate at Santiaguito volcano, Guatemala. Earth Planet Sci Lett. 2012;335.216–25.

Ebmeier S, Biggs J, Mather T, Amelung F. Applicability of InSAR to tropical volcanoes: Insights from Central America. Geochem Soc Lond Spec Publ. 2013a;380(1):15–37.

Ebmeier, S, Biggs J, Mather T, Amelung F. On the lack of InSAR observations of magmatic deformation at Central American volcanoes. J Geophys Res Solid Earth. 2013b;118(5):2571–85.

Ebmeier SK, Biggs J, Muller C, Avard G. Thin-skinned mass-wasting responsible for widespread deformation at Arenal volcano. Front Earth Sci. 2014; 2.35.

Ebmeier SK, Elliott JR, Nocquet J-M, Biggs J, Mothes P, Jarrín P, Yépez M, Aguaiza S, Lundgren P, Samsonov SV. Shallow earthquake inhibits unrest near Chiles–Cerro Negro volcanoes, Ecuador–Colombian border. Earth Planet Sci Lett. 2016;450.283–91.

Euillades PA, Euillades LD, Blanco MH, Velez ML, Grosse P, Sosa GJ. Co-eruptive subsidence and post-eruptive uplift associated with the 2011–2012 eruption of Puyehue-Cordón Caulle, Chile, revealed by DInSAR. J Volcanol Geotherm Res; 2017. https://doi.org/10.1016/j.jvolgeores.2017.06.023.

Farr TG, Rosen PA, Caro E, Crippen R, Duren R, Hensley S, Kobrick M, Paller M, Rodriguez E, Roth L, Seal D, Shaffer S, Shimada J, Umland J, Werner M, Oskin M, Burbank D, Alsdorf D. The Shuttle Radar Topography Mission. Rev. Geophys. 2007;45. https://doi.org/10.1029/2005RG000183.

Feigl KL, Le Mével H, Tabrez Ali S, Córdova L, Andersen NL, DeMets C, Singer BS. Rapid uplift in Laguna del Maule volcanic field of the Andean Southern Volcanic zone (Chile) 2007–2012. Geophys J Int. 2013;196(2): 885–901.

Fournier T, Pritchard ME, Riddick SN. The frequency, duration, and magnitude of subaerial volcano deformation events: New results from Latin America and a global synthesis. Geochem Geophys Geosys. 2010;11. https://doi.org/10.1029/2009GC002558.

Funning G, Garcia A. A systematic study of global earthquake detectability using Sentinel-1 TOPS InSAR. In: FRINGE Workshop. Helsinki: European Space Agency; 2017.

Garthwaite M, Saunders S, Hu G, Parks M. Deformation at the Rabaul caldera, Papua New Guinea modelled using ALOS PALSAR and GPS time series. In: FRINGE Workshop 2017, Helsinki, Finland; 2017.

Global Volcanism Program. Volcanoes of the World, v. 4.6.0. Smithsonian Institution, Venzke, E. (ed.) [Date accessed: 20 June 2017]. 2017. https://doi.org/10.5479/si.GVP.VOTW4-2013.

Gottsmann J, De Angelis S, Fournier N, Van Camp M, Sacks S, Linde A, Ripepe M. On the geophysical fingerprint of Vulcanian explosions. Earth Planet Sci Lett. 2011;306(1):98–104.

Grainger MH. Analyse de longues séries temporelles InSAR appliqué à' un centre volcanique en déformation: Laguna del Maule (Chili). PhD thesis, Thesis, MS, Université Toulouse III. 2017.

Henderson ST, Pritchard ME. Decadal volcanic deformation in the central Andes volcanic zone revealed by InSAR time series. Geochem Geophys Geosys. 2013;14.1358–1374. https://doi.org/10.1002/ggge.20074.

Henderson, ST, Pritchard ME. Time dependent deformation of Uturuncu volcano, Bolivia constrained by GPS and InSAR measurements and implications for source models. Geosphere. 2017. In press.

Henderson ST, Delgado F, Elliott J, Pritchard ME, Lundgren PR. Decelerating uplift at Lazufre volcanic center, central Andes, from A.D. 2010 to 2016, and implications for geodetic models. Geosphere. 2017;13(5):1–17. https://doi.org/10.1130/GES01441.1.

Hickey J, Lloyd R, Biggs J, Arnold D, Mothes P, Muller C. What's causing asymmetric flank deformation at Tungurahua Volcano, Ecuador? (abstract #399). In: IAVCEI Scientific Assembly, Portland, Oregon. Portland: IAVCEI; 2017.

Hofton MA, Malavassi E, Blair JB. Quantifying recent pyroclastic and lava flows at Arenal Volcano, Costa Rica, using medium-footprint lidar. Geophys Res Lett. 2006;33.21306.

Hua H, Owen S, Yun S, Lundgren P, Fielding E, Agram P, Manipon G, Stough T, Simons M, Rosen P, Wilson BD, Poland MP, Cervelli PF, Cruz J. Integrating remote sensing data, hybrid-cloud computing, and event notifications for Advanced Rapid Imaging & Analysis. In: AGU Fall Meeting Abstracts. San Francisco: American Geophysical Union; 2013.

Hubbard BE, Sheridan MF, Carrasco-Núñez G, Díaz-Castellón R, Rodríguez SR. Comparative lahar hazard mapping at Volcan Citlaltépetl, Mexico using SRTM, ASTER and DTED-1 digital topographic data. J Volcanol Geotherm Res. 2007;160(1):99–124.

Huggel C, Schneider D, Miranda PJ, Granados HD, Kääb A. Evaluation of ASTER and SRTM DEM data for lahar modeling: A case study on lahars from Popocatépetl Volcano, Mexico. J Volcanol Geotherm Res. 2008;170(1): 99–110.

Iguchi M, Yakiwara H, Tameguri T, Hendrasto M, Hirabayashi J-i. Mechanism of explosive eruption revealed by geophysical observations at the Sakurajima, Suwanosejima and Semeru volcanoes. J Volcanol Geotherm Res. 2008;178(1):1–9.

Jay JA, Welch M, Pritchard ME, Mares PJ, Mnich ME, Melkonian AK, Aguilera F, Naranjo JA, Sunagua M, Clavero J. Volcanic hotspots of the central and southern Andes as seen from space by ASTER and MODVOLC between the years 2000-2010. In: Pyle D, Mather TA, Biggs J, editors. Remote Sensing of Volcanoes and Volcanic Processes: Integrating Observation and Modelling. London: Geological Society of London; 2013. p. 161–185.

Jay JA, Delgado FJ, Torres JL, Pritchard ME, Macedo O, Aguilar V. Deformation and seismicity near Sabancaya volcano, southern Peru, from 2002 to 2015. Geophys Res Lett. 2015;42(8):2780–8.

Jay J, Costa F, Pritchard M, Lara L, Singer B, Herrin J. Locating magma reservoirs using InSAR and petrology before and during the 2011–2012 Cordón Caulle silicic eruption. Earth Planet Sci Lett. 2014;395.254–66.

Johnson JB, Lyons J, Andrews B, Lees J. Explosive dome eruptions modulated by periodic gas-driven inflation. Geophys Res Lett. 2014;41(19):6689–97.

Krotkov NA, Carn SA, Krueger AJ, Bhartia PK, Yang K. Band residual difference algorithm for retrieval of SO/sub 2/from the aura ozone monitoring instrument (OMI). IEEE Trans Geosci Remote Sens; 2006;44(5): 1259–66.

Kubanek J, Westerhaus M, Heck B. Topographic changes at Volcan de Colima observed by double differential InSAR using TanDEM-X. In: Proceedings of ESA Living Planet Symposium 2013, Edinburgh, Scotland. SP=722. Helsinki: European Space Agency; 2013.

Le Mével H, Feigl KL, Córdova L, DeMets C, Lundgren P. Evolution of unrest at Laguna del Maule volcanic field (Chile) from InSAR and GPS measurements, 2003 to 2014. Geophys Res Lett. 2015;42(16):6590–8.

Liang C, Fielding EJ. Measuring azimuth deformation with L-band ALOS-2 ScanSAR interferometry. IEEE Trans Geosci Remote Sens. 2017. https://doi.org/10.1109/TGRS.2017.2653186.

Lipman PW, Mullineaux DR, Vol. 1250. The 1980 Eruptions of Mount St. Helens, Washington. Washington, D.C: US Dept. of the Interior, US Geological Survey; 1981.

Londono JM. Evidence of recent deep magmatic activity at Cerro Bravo-Cerro Machín volcanic complex, central Colombia. Implications for future volcanic activity at Nevado del Ruiz, Cerro Machín and other volcanoes. J Volcanol Geotherm Res. 2016;324.156–68.

López JF, Barbero I, Viramonte JG, Velez ML, Euillades L, Blanco M. Deformation pattern on Cerro Blanco Volcanic Complex (CBVC). In: Cities on Volcanoes Conference, vol. 9. Puerto Varas: IAVCEI; 2016. p. 138.

Lundgren P, Samsonov SV, López Velez CM, Ordoñez M. Deep source model for Nevado del Ruiz Volcano, Colombia, constrained by interferometric synthetic aperture radar observations. Geophys Res Lett. 2015;42(12): 4816–23.

Pritchard *et al. Journal of Applied Volcanology*   (2018) 7:5

Page 27 of 28

Lundgren P, Nikkhoo M, Samsonov SV, Milillo P, Gil-Cruz F, Lazo J. Source model for the Copahue volcano magma plumbing system constrained by InSAR surface deformation observations. J Geophys Res Solid Earth. 2017;122.5729–47. https://doi.org/10.1002/2017JB014368.

Mahmood A. RADARSAT-1 background mission implementation and accomplishments. Can J Remote Sens. 2014;40(6):385–95.

McCormick BT, Edmonds M, Mather TA, Carn SA. First synoptic analysis of volcanic degassing in Papua New Guinea. Geochem Geophys Geosyst. 2012;13(3).

Morales-Rivera A, Amelung F, Mothes P, Hong S-H, Nocquet J-M, Jarrin P. Ground deformation before the 2015 eruptions of Cotopaxi volcano detected by InSAR. Geophys Res Lett; 2017. https://doi.org/10.1002/2017GL073720.

Morales-Rivera M, Anieri, Amelung F, Mothes P. Volcano deformation survey over the northern and central Andes with ALOS InSAR time series. Geochem Geophys Geosyst. 2016;17(7):2869–83.

Moran SC, Newhall C, Roman DC. Failed magmatic eruptions: Late-stage cessation of magma ascent. Bull Volcanol. 2011;73(2):115–22.

Moreno H, Clavero J. Geología del área del volcán Villarrica, 1: 50,000. Carata Geológica de Chile, Serie Geología Básica. 2006;98.

Muller CS. Integrated volcano geodesy: Application to Arenal, Costa Rica and Tungurahua, Ecuador. PhD thesis, PhD Thesis, University of Bristol, UK. 2016.

Muller C, del Potro R, Biggs J, Gottsmann J, Ebmeier SK, Guillaume S, Cattin P-H, Van der Laat R. Integrated velocity field from ground and satellite geodetic techniques: application to Arenal volcano. Geophys J Int. 2015;200(2):863–79.

Naranjo MF, Ebmeier SK, Vallejo S, Ramón P, Mothes P, Biggs J, Herrera F. Mapping and measuring lava volumes from 2002 to 2009 at El Reventador Volcano, Ecuador, from field measurements and satellite remote sensing. J Appl Volcanol. 2016;5(1):1–11.

Newhall C, Aramaki S, Barberi F, Blong R, Calvache M, Punongbayan J-LCR, Siebe C, Simkin T, Sparks S, Tjetjep W. Professional conduct of scientists during volcanic crises. Bull Volcanol. 1999;60(5):323–34.

Nikkhoo M, Walter TR, Lundgren PR, Prats-Iraola P. Compound dislocation models (cdms) for volcano deformation analyses. Geophys J Int. 2017;208(2):877–94.

Nobile A, Smets B, d'Oreye N, Geirsson H, Samsonov S, Kervyn F. InSAR and GPS ground deformation measurements to characterize the Nyamulagira magma plumbing system during the 2011-2012 volcanic eruption. In: FRINGE Workshop 2017, Helsinki. Helsinki: European Space Agency; 2017.

Pallister JS, Schneider DJ, Griswold JP, Keeler RH, Burton WC, Noyles C, Newhall CG, Ratdomopurbo A. Merapi 2010 eruption—Chronology and extrusion rates monitored with satellite radar and used in eruption forecasting. J Volcanol Geotherm Res. 2013a;261.144–52.

Pallister JS, Diefenbach AK, Burton WC, Munoz J, Griswold JP, Lara LE, Lowenstern JB, Valenzuela CE. The Chaitén rhyolite lava dome: Eruption sequence, lava dome volumes, rapid effusion rates and source of the rhyolite magma. Andean Geol. 2013b;40(2):277–94.

Parker AL, Biggs J, Walters RJ, Ebmeier SK, Wright TJ, Teanby NA, Lu Z. Systematic assessment of atmospheric uncertainties for InSAR data at volcanic arcs using large-scale atmospheric models: Application to the Cascade volcanoes, United States. Remote Sens Environ. 2015;170.102–14.

Passarelli L, Brodsky EE. The correlation between run-up and repose times of volcanic eruptions. Geophys J Int. 2012;188(3):1025–45.

Pavez A, Remy D, Bonvalot S, Diament M, Gabalda G, Froger J-L, Julien P, Legrand D, Moisset D. Insight into ground deformations at Lascar volcano (Chile) from SAR interferometry, photogrammetry and GPS data: Implications on volcano dynamics and future space monitoring. Remote Sens Environ. 2006;100(3):307–20.

Pavolonis MJ, Sieglaff J, Cintineo JL. Automated utilization of weather satellites for global mitigation of aviation related volcanic hazards (abstract). In: Aviation, Range, and Aerospace Meteorology Special Symposium, 5th, and Conference on Environmental Information Processing Techniques, 32nd, New Orleans, LA, 10-14 January 2016; 2016.

Pepe S, Castaldo R, De Novellis V, D'Auria L, De Luca C, Casu F, Sansosti E, Tizzani P. New insights on the 2012-2013 uplift episode at Fernandina volcano (Galápagos). Geophys J Int. 2017;211(2):695–707.

Percivall GS, Alameh NS, Caumont H, Moe KL, Evans JD. Improving disaster management using earth observations—GEOSS and CEOS activities. IEEE J Sel Top Appl Earth Obs Remote Sens. 2013;6(3):1368–75.

Phillipson G, Sobradelo R, Gottsmann J. Global volcanic unrest in the 21st century: An analysis of the first decade. J Volcanol Geotherm Res. 2013;264. 183–96.

Pieri D, Abrams M. ASTER observations of thermal anomalies preceding the april 2003 eruption of Chikurachki volcano, Kurile Islands, Russia. Remote Sens Environ. 2005;99(1):84–94.

Pinel V, Poland MP, Hooper A. Volcanology: Lessons learned from synthetic aperture radar imagery. J Volcanol Geotherm Res. 2014;289.81–113.

Poland MP. Time-averaged discharge rate of subaerial lava at Kīlauea volcano, Hawai'i, measured from TanDEM-X interferometry: Implications for magma supply and storage during 2011–2013. J Geophys Res Solid Earth. 2014;119(7):5464–81.

Potin P, Rosich B, Roeder J, Bargellini P. Sentinel-1 mission operations concept. In: Geoscience and Remote Sensing Symposium (IGARSS), 2014 IEEE International. Quebec City: IEEE; 2014. p. 1465–1468.

Ramsey MS. Synergistic use of satellite thermal detection and science: a decadal perspective using ASTER. Geol Soc London Spec Publ. 2016;426(1): 115–36.

Richter N, Salzer JT, de Zeeuw-van Dalfsen E, Perissin D, Walter TR. Constraints on the geomorphological evolution of the nested summit craters of Láscar volcano from high spatio-temporal resolution TerraSAR-X interferometry. Bull Volcanol. 2018;80.21. https://doi.org/10.1007/s00445-018-1195-3.

Rivera A, Zamora R, Uribe J, Wendt A, Oberreuter J, Cisternas S, Gimeno F, Clavero J. Recent changes in total ice volume on volcán Villarrica, southern Chile. Nat Hazards. 2015;75(1):33.

Roman DC, La Femina PC, Connor C, Connor L, Dixon TH, Feineman MD, Gallant E, Geirsson H, Glover C, Rinehart JM, Ruiz G, Saballos A, Strauch W, Tenorio V, Wauthier C, Webley PW, Wnuk K. Multidisciplinary Studies of the 2015-2016 Eruption of Momotombo Volcano, Nicaragua. AGU Fall Meet Abstr; 2016.

Rose WI, Palma JL, Wolf RE, Gomez ROM. A 50 yr eruption of a basaltic composite cone: Pacaya, Guatemala. Geol Soc Am Spec Pap. 2013;498. 1–21.

Sacco P, Daraio MG, Battagliere ML, Coletta A. Mitigation of volcanic risk: the COSMO-SkyMed contribution. In: FRINGE Workshop 2015, ESA-ESRIN. Frascati: European Space Agency; 2015.

Salvi S. The GEO Geohazard Supersites and Natural Laboratories - GSNL 2.0: improving societal benefits of Geohazard science. In: EGU General Assembly Conference Abstracts, vol. 18. Vienna: European Geosciences Union; 2016. p. 6969.

Salzer JT, Nikkhoo M, Walter TR, Sudhaus H, Reyes-Dávila G, Bretón M, Arámbula R. Satellite radar data reveal short-term pre-explosive displacements and a complex conduit system at Volcán de Colima, Mexico. Front Earth Sci. 2014;2.12.

Schaefer LN, Lu Z, Oommen T. Post-eruption deformation processes measured using ALOS-1 and UAVSAR InSAR at Pacaya Volcano, Guatemala. Remote Sens. 2016;8(1):73.

Solano-Rojas D, Wdowinski S, Amelung F, Cabral-Cano E, Zhang Y, Walter T. InSAR monitoring of the Popocatépetl Volcano in central Mexico. In: FRINGE Workshop. Helsinki: European Space Agency; 2017.

Solikhin A, Pinel V, Vandemeulebrouck J, Thouret J-C, Hendrasto M. Mapping the 2010 Merapi pyroclastic deposits using dual-polarization Synthetic Aperture Radar (SAR) data. Remote Sens Environ. 2015;158.180–92.

Spaans K, Hatton E, Gonzalez P, Walters R, McDougall A, Wright T, Hooper A. Tectonic and volcanic monitoring using Sentinel-1: Current status and future plans of the COMET InSAR portal. In: EGU General Assembly Conference Abstracts. Vienna: European Geosciences Union; 2017. p. 19397.

Stephens KJ, Wauthier C. Satellite geodesy captures offset magma supply associated with lava lake appearance at Masaya volcano, Nicaragua. Geophys Res Lett. 2018;45. https://doi.org/10.1002/2017GL076769.

Stephens KJ, Ebmeier SK, Young NK, Biggs J. Transient deformation associated with explosive eruption measured at Masaya volcano (Nicaragua) using Interferometric Synthetic Aperture Radar. J Volcanol Geotherm Res. 2017;344.212–23.

Stix J. Stability and instability of quiescently active volcanoes: The case of Masaya, Nicaragua. Geology. 2007;35(6):535–8.

Tait S, Ferrucci F. A real-time, space borne volcano observatory to support decision making during eruptive crises: European Volcano Observatory Space Services. In: Computer Modelling and Simulation (UKSim), 2013 UKSim 15th International Conference On. Cambridge: IEEE; 2013. p. 283–9.

Pritchard *et al. Journal of Applied Volcanology* (2018) 7:5

Page 28 of 28

Velez M, Euillades P, Blanco M, Euillades L. Ground deformation between 2002 and 2013 from InSAR observations. In: Tassi F, Vaselli O, Caselli AT, editors. Copahue Volcano. Berlin: Springer; 2016. p. 175–98.

Voight B, Sparks R, Miller A, Stewart R, Hoblitt R, Clarke A, Ewart J, Aspinall W, Baptie B, Calder E, et al. Magma flow instability and cyclic activity at Soufriere Hills Volcano, Montserrat, British West Indies. Science. 1999;283(5405):1138–42.

Wadge G, Cole P, Stinton A, Komorowski J-C, Stewart R, Toombs A, Legendre Y. Rapid topographic change measured by high-resolution satellite radar at Soufriere Hills Volcano, Montserrat, 2008–2010. J Volcanol Geotherm Res. 2011;199(1):142–52.

Wauthier C. Volcano geodesy. In: Workshops on Volcanoes 2016, Quetzaltenango, Guatemala; 2016.

Wicks C, de la Llera JC, Lara LE, Lowenstern J. The role of dyking and fault control in the rapid onset of eruption at Chaitén volcano, Chile. Nature. 2011;478.374–7.

Wnuk K, Wauthier C. Temporal evolution of surface deformation and magma sources at Pacaya Volcano, Guatemala revealed by InSAR. J Volc Geotherm Res; 2017. https://doi.org/10.1016/j.jvolgeores.2017.06.024.

Wright R, Flynn LP, Garbeil H, Harris AJL, Pilger E. MODVOLC: near-real-time thermal monitoring of global volcanism. J Volc Geotherm Res. 2004;135. 29–49.

Wulder MA, Hilker T, White JC, Coops NC, Masek JG, Pflugmacher D, Crevier Y. Virtual constellations for global terrestrial monitoring. Remote Sens Environ. 2015;170.62–76.

Xu W, Jónsson S, Ruch J, Aoki Y. The 2015 Wolf volcano (Galápagos) eruption studied using Sentinel-1 and ALOS-2 data. Geophys Res Lett. 2016;43(18): 9573–80.